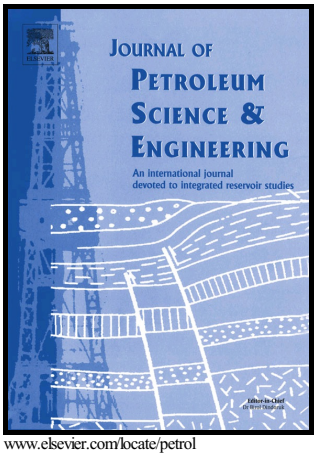

www.elsevier.com/locate/petrol

Petrophysical evaluation and uncertainty analysis of Roseneath and Murteree shales reservoirs in Cooper Basin, Australia (a case study)

Quaid Khan Jadoon, Eric Roberts, Thomas Blenkinsop, Raphael A.J. Wust, Syed Anjum Shah

PII: S0920-4105(16)30231-5
DOI: http://dx.doi.org/10.1016/j.petrol.2016.06.010
Reference: PETROL3501

To appear in: *Journal of Petroleum Science and Engineering*

Received date: 19 August 2015
Revised date: 3 June 2016
Accepted date: 7 June 2016

Cite this article as: Quaid Khan Jadoon, Eric Roberts, Thomas Blenkinsop Raphael A.J. Wust and Syed Anjum Shah, Petrophysical evaluation and uncertainty analysis of Roseneath and Murteree shales reservoirs in Coope Basin, Australia (a case study), *Journal of Petroleum Science and Engineering* http://dx.doi.org/10.1016/j.petrol.2016.06.010

Petrophysical evaluation and uncertainty analysis of Roseneath and Murteree shales reservoirs in Cooper Basin, Australia (a case study)

Quaid Khan Jadoon[1*], Eric Roberts[1], Thomas Blenkinsop[1], Raphael A.J. Wust[1,2], Syed Anjum Shah[3]

[1]Department of Earth and Oceans James Cook University Townsville Queensland, Australia

[2]TRICAN Geological Solutions Ltd. 621- 37th Avenue N.E Calgary, Alberta, Canada

[3]Saif Energy Limited Street, 34, House No, 12, F7/1 Pakistan

Abstract

This study investigates petrophysical characteristics of lacustrine Permian Murteree and Roseneath shales in relation to reservoir evaluation of the most prospective gas shale plays in the Cooper Basin, Australia. Both shales were investigated for gas volumes by employing unconventional petrophysical techniques through a combination of source rock parameters acquired by geochemical analysis, and integrating the extracted parameters into log interpretation and core studies. Modeling mineralogical composition using wireline logs require the selection of a proper mineral model. In this study, the mineral model was built in the Interactive Petrophysics (IP's) Mineral Solver module by integrating all regional sedimentological, petrographic, SEM (Scanning electronic microscope), pulse decay and X-ray diffraction data (XRD) from core and chip cutting samples. This study developed a mineral grouping framework to assist in the selection of a proper model to easily solve complex shale gas reservoirs for gas volumes. Furthermore, the permeability of both shales depends on in-situ confining stress and permeability of these cores and can be calculated through decay rate of a pressure pulse applied to experimental data. Subsequent to the integrated study as explained above, it is concluded on the basis of extruded parameters (shale porosity, permeability, volume of kerogen, volume of brittle minerals and water saturation) that Murteree formation exhibits better potential than Roseneath formation in and around Nappameri, Patchawarra and Tenappera troughs, while poor potential is exhibited in the Allunga trough. The only location where Roseneath exhibits better potential is in Encounter-01 well.

Key words: Shale gas, Roseneath, Murteree, Petrophysical, Mineral model, TOC, XRD.

Introduction

Advancements in drilling and well completion techniques over the last 20 years have resulted in the exploration of many unconventional liquid and gas reservoirs around the globe (Wust et al., 2015). Unconventional hydrocarbon reservoirs differ from conventional reservoirs in that they commonly represent both source and reservoir for hydrocarbon- generation and accumulation. During burial and diagenesis, some hydrocarbons may be lost due to migration, but much remains in place due to the low permeability of the host rock (Myers, 2008). To date, the vast bulk of unconventional shale gas has been developed in North America, with the minimal exploitation of this resource in other parts of the world (e.g. S-America, China, Europe, and Australia).

The Cooper Basin (Fig. 1) is widely regarded as one of the most prospective basins in Australia for shale gas. Its sedimentary succession hosts a significant amount of Australia's onshore oil and gas, which has been in production, mainly for natural gas (with some liquids), since 1963. The basin is the largest onshore petroleum province in Australia (Hill and Gravestock, 1995) and has both conventional and unconventional reservoirs. The main hydrocarbon reservoir intervals in the basin are located within the Late Paleozoic Gidgealpa Group (Fig. 2).

After Santos successfully started gas production at the Moomba-191 in shale gas reservoirs, unconventional exploration expanded and various companies, including Beach Energy, Senex, Drillsearch, Strike Energy, Santos and a number of joint ventures, initiated shale and tight gas and oil exploration and evaluation programs in Cooper Basin. The exploration and exploitation history in the Cooper Basin means that significant infrastructure for gas exploitation is already present, which is advantageous to the development of shale gas and gas shale reservoirs. There are three main prospective deep troughs present in the basin which has the greatest unconventional oil and gas potential; the troughs are Nappamerri, Patchawara and Tenappera troughs (PESA, 2014).

Since earlier exploration concentrated on conventional clastic and carbonate reservoirs, only conventional logging was used to investigate the potential of conventional reservoirs. The logs include gamma ray, resistivity, neutron-density, and sonic log, with limited formation tests

and rotary sidewall coring (Vallee, 2013). However, shale gas formation evaluation requires more than the logs available in the basin. Luckily, a small number of cores for the Roseneath and Murteree formations are available in the core archive of Department for Manufacturing, Innovation, Trade, Resources and Energy by the Government of South Australia (DMITRE).

The DMITRE cores from the Murteree and Roseneath shale intervals and wireline logs were interpreted in this study to evaluate the potential for lacustrine shale gas reservoirs in the Cooper Basin. Integration of cores and logs are presented in Table. 1-2. The following parameters were taken from both core/cuttings and logs and matched with each other in order to get these parameters from top to bottom of the formation. Total organic carbon content (TOC) from pyrolysis, powder x-ray diffraction (XRD), permeability(pulse decay) porosity, grain density and water saturation (S_w) data were all measured and compiled in this project.

The primary aims of this study are: 1) to determine the shale gas potential of lacustrine shale by estimating organic content, mineral content, porosity and permeability of the Roseneath and Murteree shales; 2) to make a mineral and petrophysical model which can be used to help analyse and evaluate nearby wells ; 3) to measure permeability from same core plugs; 4) to investigate the petrography and perform SEM analysis of selected core samples for mineralogical analysis; and 5) to develop a simple workflow which can be adapted even with handful of conventional logs.

Methodology

This study presents an integrated analysis of drill core, wireline logs, geochemistry and XRD, which are utilized in the mineral and petrophysical modeling presented below. Wireline data, including gamma ray (GR), sonic (DT), density (Rhob), Photo electric effect (PEF) neutron(NPHI) and resistivity (MSFL, LLS, LLD) logs and drill core samples collected from twenty one wells in the Nappameri, Allunga, and Tenappera troughs were available for study. Core plugs were sampled and quality checked at the Department of Manufacturing, Innovation, Trade, Resources and Energy (DIMITRE) South Australia and Queensland Department of Natural Resources and Mines core library facilities (DNRM). Wireline data (Log ASCII Standard-LAS files) for GR, Rhob, PEF, Nphi, DT and MSFL, LLS, LLD records were loaded into IP 4.3 (Interactive

petrophysics) Senergy software, first edited/reviewed and then integrated with core and cutting data for mineral modeling recognition in the intersections of the Roseneath and Murteree shales in exploration wells.

Detailed methodology of mineral modeling is reported in (Jadoon et al., 2016), this study further extends the mineral modeling methodology to calculate the volume of kerogen along with lithology volumes in wells having a complete log and core data and then this methodology extends this to wells having limited data with the help of parameters taken from wells having full data. All sample location information, including formation, well, stratigraphic position and types of analyses performed for each sample are provided in Appendix-1. Petrophysical properties estimated include shale porosity, permeability, water saturation, kerogen, mineral volumes and CEC are reported in (Tables 3-4).

The database is divided into key and non-key wells according to data available. The wells which had full logs and core data were termed key wells and the wells having limited data were termed non-keys wells (Table-02). The parameters of key wells were used in non-keys wells to extend the approach defined in all wells across the basin. Table-01 shows which information we can get from which kind of data. Below are the steps which are necessary to perform any multiple mineral modeling for evaluation of gas shale reservoirs.

First re-normalize the XRD and TOC weight percent values so that all the minerals and organic content sums to 100%. Then convert weight percent to volume percent by equation 1,

WVP = (DW%) * (1-PHIT) * (RGD)/ (MGD)……1

Where,

WVP = Wet volume percent, DW% = Dry Weight %), PHIT= Total Porosity, RGD = Rock Grain Density, MGD = Mineral Grain Density.

Use rock grain density and porosity from the routine core analysis. If a porosity measurement doesn't consist of enough data points (as the case of this project) then it is first needed to calculate porosity and match with core sample before converting weight percent to volume percent. The details of porosity quantification and eradication of clay and kerogen effects from the porosity are given in the porosity quantification in detail. The

conversion from weight to volume percent can be done by using the mineral solver processing utility in the software package (IP4.3), which converts weight percent into volume percent using the equation 1. After conversion, put kerogen as a separate mineral along with dominant and auxiliary minerals to solve for its volumes. Common default values of kerogen density are between 1.3 to 1.35 g/cc, so 1.30 g/cc density for kerogen was used consistently in the project. It is ensured that the output curves don't exceed the input curves because software can't solve more minerals than input curves. The default values for minerals are set to those that have been put in the mineral solver. Finally, set parameters for S_w before running the model for several iterations until a fair match is achieved between the XRD volume percent and mineral solver output and input curves.

Water saturation has been calculated by the classical shaly sand equations i.e, Dual water equation (Clavier et al., 1977), Waxman Smit's equation (Waxman and Smits, 1968) and Juhasz's equation (Juhasz et aI., 1981, Normalized Qv). After attaining reasonable match between log and core outputs, the parameters and approach specified above has been used in evaluating the adjoining wells with no core data.

The Permeability of the core is calculated through decay rate of a pressure pulse applied. Sample preparation included cutting, grinding, drying and pre-stressing, which has been conducted at Trican Lab Calgary Canada. All the measurements have been using helium as a test gas (Cui et al., 2009; Kowalczyk et al., 2010). The pulse decay method involves creating an instant pressure difference or pulse commonly less than 50 psi between the upstream and downstream reservoirs a tightly jacketed core plug in a biaxial core holder. The decay of the initial pressure pulse is monitored with time and used to calculate the permeability along the axis of the core plugs. Pore pressure of samples is maintained at about 1000 psi to reduce the gas diffusion effects. Increasing confining pressure that imitates the in-situ reservoir stress path can be applied to the jacketed samples in the core holder and the corresponding permeability is then measured. While the sample was under compressive stress the pulse decay permeater was used to measure the permeability of cut samples at certain confining pressures and flow rates.

Quantification of porosity:

Since very few core porosity data points were available for the project, a log-derived porosity curve was created from the density curve. This curve was then used in the transformation of XRD weight percent to volume percent. TOC remains indistinguishable from porosity on the density log in organic shales (Cluff, 2012). A kerogen correction needed to be applied to the porosity computed with density log because the conventional method can lead to overestimation of porosity. Better porosity estimates were computed either by density log or by stochastic well log interpretation. Porosity was computed for conversation of weight percent to volume percent density method. Then the porosity was computed with following density log equations (Krygowsk, 2003).

$\phi D = (\rho M - \rho B) / (\rho M - \rho F)$

Where

ϕD = Density porosity

ρM = Matrix density

ρB = Bulk density from the density Log

ρF = Fluid density

Porosity correction for Kerogen

$\phi DKC = \phi D - (VKF * \phi DK)$

Where,

ϕDKC = Density porosity corrected for kerogen content.

ϕDK = Density porosity of kerogen.

VKF= Volume of Kerogen in fraction

Mineral Modeling Methods

A mineral model is necessary for understanding any gas shale reservoir. It helps to quantify each mineral's volume present from top to bottom of a reservoir, providing indications of brittleness and ductile nature of reservoir, in addition to prospectivity. It helps to correct the

porosity from extreme clay and kerogen effects. Evaluation of shale gas reservoirs can be done by integration of the XRD, wireline logs and geochemical data (Bust, 2011). This can be achieved by performing XRD analysis on core or cutting data, which can be matched with the log-driven mineral volumes output to get a consistent litho-curve in volume percent from top to bottom of a reservoir. In stochastic approach, models can be used in adjoining wells because of the utility of reconstruction curves which are reconstructed from the built petrophysical and mineral model. If the input curves and reconstructed curves match well then it gives an assurance that the model is appropriate for that region too. If it doesn't match then reiteration can be done to match them.

Shale units of REM (Roseneath Epsilon Murteree) consist of about 10 or so essential and auxiliary minerals, including predominant minerals like quartz, carbonates, feldspar, titanium-oxides, illite, kaolinite and muscovite. Only four log measurements were available for most of the wells, although a few wells had complete conventional log suites. The limitation with multiple mineral analyses that it can't solve more minerals than the number of input curves handicapped the analysis because 4-5 mineral curves were present for most of the wells. So, in order to solve the formation having 10 minerals, the mineral should have to be grouped on the basis of their genesis to proper evaluation of reservoirs. The grouping was done on the basis of the genesis of the minerals constituents. For Example, muscovite and chlorite were grouped in illite mineral because illite was dominant amongst the clay minerals. Albite and K-feldspar were grouped with quartz mineral because of two reasons, quartz was the most dominant mineral amongst brittle minerals and the proportion of albite and K-feldspar was nominal. Mg-siderite was grouped in siderite mineral because both are carbonates. Tri-oxides being brittle minerals were grouped with other brittle oxide minerals. Two different approaches were used to make two different models for this study due to data constraints. For wells having all conventional log suits available, mineral volumes for quartz, siderite, illite/mica, kaolinite and kerogen were calculated separately (Figs. 3-5). For wells having only sonic, resistivity and GR logs, the brittle minerals were grouped as one mineral and the clay minerals were grouped as another mineral along with kerogen as a separate mineral (Fig.6). For wells having limited data, adjoining mineral model was used to solve for S_w if there was full conventional log data (Fig.7). The sensitivity of sonic logs to textures rather than volumes skewed the process but the

reconstructed curves utility of multiple minerals was used to validate the model. The mineral model was validated by the direct comparison of mineral compositions obtained by XRD analysis of the core, which was later transformed to volume percent.

Results and Discussion

The results for both Roseneath and Murteree formations have been tabulated in the table (Table 3). Average porosity, clay volume, total organic content, water saturation and permeability are presented. The averages of properties measured indicate that Murteree Formation exhibits better potential in terms of S_w. The porosity and TOC are significant in both the formations in Allunga and Tennapera troughs which can be conductive for harbouring of adsorb gas. Grouping of minerals on the basis of their genesis has provided a good means for making of a reliable mineral and petrophysical model which give favourable results in terms of required properties. The stochastic mineral models provide the best means to calculate the tabulated properties (Bust et al., 2011 and Ramez et al., 2011).

Plug permeability measurements

The permeability of Roseneath and Murteree was measured at pore pressure of (10- 70 Mpa) (1400-990 psi). Pulse Decay permeability (PDP) data is presented from Roseneath and Murteree shales samples Dirkala-2, Encounter-1 and Ashby-1 wells (Appendix-1 Table.7). Permeability provides an indication of matrix permeability but does not account for large scale fabric or microfractures. Permeability measured on sample plugs under confining stress with pressure -pulse-decay shows a large spread in permeability with several orders of magnitude differences between the lowest and the highest samples (Figs 8-10). Roseneath and Murtreee shales samples were measured perpendicular to bedding plane direction. The samples are in outlier and after testing, showed a marked fracture network that developed under confined pressure. Roseneath Shale in Encounter well confining pressure from 23.77- 61.44 Mpa (23.77-61.44 Mpa). The Helium gas pressure 20 to 1024 psi (0.14 to 692 Mpa). In Murteree Shale Dirkala-2 confining pressure from 1400 to 5838 psi (9.65 – 40.25Mpa), while in Ashby confining pressure 2426 to 6390 psi (16.75- 44.06 Mpa). The Helium gas pressure in Murteree 993 to 1042 psi (6.85 to 7.19 Mpa). These data were fit to an effective stress law. The permeability

under stress results for the Encounter-1, Dirkala-2 and Ashby-1 wells were selected for variation. Permeability versus modified effective stress is plotted in (Figs. 8-10) using the same effective stress law for each sample. Most of the samples less than 1md indicating the rocks are more sensitive to changes in pore pressure. Noting that permeability as a function of modified effective stress forms a trend enables us to attribute all permeability variation observed >1000 psi (7.4 Mpa). Permeability units for samples Encounter-1, Dirkala-2, Ashby-1, are in milidarcy range. All the wells lie less than 1 md except Tirrawara-2(Fig. 11). In Petrophysical model the log derived permeability in Dikala-2, Ashby-01, and Encounter-1 match very well with core measured permeability. It was estimated by Coates equation.

Resistivity of Water:

Formation water resistivity (R_w) was computed by a combination of SP, apparent water resistivity calculated from logs and Picket cross-plots (Figs. 12 -13). A minimum value of R_w for both the formations was used because the determinations of the shale-gas potential of the Roseneath and Murteree formations are at the initial phase. An optimistic approach was followed to begin with since the projects are large scale. Generally, in the Permian shale wells in this study area R_w corresponds to a water salinity of 6000-8000 ppm Nacl. It also match to the regional R_w from analyses of water from drill stem tests that are taken from the well completion reports of Ashbay-01, Dirkala-01, 02, Encounter-01.

Water Saturation:

Water saturation is generally computed by the conventional Archie approach which requires total porosity, resistivity, R_w, m, n and a .There is no assurance that the rocks being analyzed act like Archie or shaly-sand systems (Cluff, 2012). The water saturation (S_w) for this project is calculated by using the standard shaly sand equations, which include the Waxman-Smits equation (Waxman and Smits, 1968), the Dual Water equation (Clavier, 1977; Coates and Dumanoir, 1984) and the Juhasz equation Normalized Q_v (Juhasz, et., 1981).None of these equations can be considered as 'the best' equation since such equations tend to give better results in some situations rather than others and usually for unknown reasons. The Juhasz equation was selected initially because no Cation Exchange Capacity (CEC) data from core

samples were available. In the absence of special core analysis, (SCAL) Q_v can be calculated by logs through Juhasz's method and replaced in the W-S equation. The Q_{vn} is defined as normalized Q_v: $Q_v = Q_{vn}/ Q_v$ shl.

The use of Juhasz's equation includes the assumption that the approach can be applicable to formations of constant salinity and clay mineralogy; the zones conforming to the assumptions specified above are facilitated by pattern recognition based on Q_v(cation exchange capacity per unit total pore volume)and log response in general (Juhasz et al., 1981, Normalized Qv),(Figs.15 and 16). Historically Q_v has been calculated by core data and is correlated with some appropriate logs in order to define the Q_v profile over the hydrocarbon bearing sections. Here it was correlated with porosity and a linear relationship between Q_v total porosity (ϕT) was observed, which was extended to the hydrocarbon bearing sections.

The dispersed clay (generally clay and usually authigenic), laminated clay/shale (probably shale), and structural clay (shale rip-up clasts) were assumed not to affect the estimation of total porosity (ϕT) and water saturation (S_w).The shale gas petrophysical models define the existence of additional conductivity due to clay surface Cation Exchange Capacity (CEC) to the conductivity due to normal brine in the reservoirs. The additional conductivity exerts adverse effects when the water in the formation is relatively fresh. The S_w calculations are very sensitive to the additional conductivity measurements (Waxman and Smits, 1968). The additional conductivity is usually shown in terms of the Cation Exchange Capacity normalised to the total pore volume (Q_v) (Waxman and Smits, 1968).

Where,

a = tortuosity factor

m = cementation factor

n = saturation exponent

Replacing Qv with log data:

The derived Q_v or pore volume concentration of clay exchange cations (meq/mL) was then correlated with total porosity (ϕT) in order to define the Q_v -profile over the hydrocarbon bearing sections for calculation of S_w. Q_v -total porosity (ϕT) correlations have been used in the past for validation of Q_v values so it was used in the model (Juhaz,1971).The parameter B (equivalent conductance of the Na^+ exchange cations $mho.m^{-1}$/ $meq.com^{-3}$) has been experimentally defined by Waxman and Thomas to be a function of salinity and temperature. The approximate values can be computed by the expression (Waxman et al., 1974)

$$B = -1.28 + 0.225t - 0.0004059t^2/1 + R_w^{\,1\cdot23}\,(0.045t - 0.27)$$

Where t is in °C and R_w in ohm.m.

Juhasz 1971 clearly illustrates that BQ_v computed for any shale volume is the difference between the two water conductivities or the apparent water conductivity of the water-bearing shaly sand and the conductivity of the formation water. Knowing B, Q_v can be calculated by the following equation with the help of resistivity and porosity logs,

$$Q_v = C_{we} - C_w /B = 1/B\ (\phi\text{-}m /Ro - 1/ R_w)$$

This approach has been successfully used when there is no core derived CEC is available (Juhasz et al., 1981).Qv obtained from this equation was then plotted (Fig. 14) against the corresponding total porosity (ϕT) in order to define a Q_v - ϕT relationship either in the form of

$$Q_v = a\ \phi T\ \text{^-}b$$

Or $Q_v = a/\phi T - b$

Where 'a' and 'b' are the entered Q_v a and b constant parameters taken from the cross-plot (Figs. 14) since the true relationship between Q_v and ϕT is a reciprocal, (Q_v = CEC/PV), the Q_v – $1/\phi T$ plot is always a straight line in shales where it meets the assumption specified above (Juhasz et al., 1981). A linear relation between Q_v and $1/\ \phi T$ was observed on the cross-sections (Fig. 14) in water zone.

Petrography and SEM of the Roseneath and Murteree shales

On the basis of detailed petrographic analysis of the Permian Murteree and Roseneath shales, discrete mineralogy has been recognized in this study. Thin section and SEM descriptions focus on the morphology of mineralogy, texture, quartz-mud ratio and kerogen. The kerogen is classified on the basis of maceral analysis in the Roseneath and Murteree shales in Cooper Basin are generally thought to have originated from the abundant dispersed organic matter (3 to 6% TOC wt) (Jadoon et al., 2016). The Roseneath and Murteree shales are very heterogeneous formations. Clay-rich intervals with coal interbeds can easily be identified by visual inspection of the core. XRD analysis demonstrates that both shales primarily contain clay minerals; kaolinite, illite, muscovite and quartz (Appendix-1). The shales are composed mainly of clay, authigenic quartz, siderite and kerogen. Thin section images show that organic matter is present and aligned parallel to bedding planes accounting for the TOC (as determined from logs and core). SEM and thin section analyses provide much needed visual evidence to understand how the porosity and fractures are distributed at the micro-scale.

Uncertainty analysis:

Uncertainty analysis was used to estimate the errors in a petrophysical analysis. The petrophysical analysis was aided with the most reliable core studies, most of the core derived parameters (mineral constituents, porosity, TOC, permeability) were matched with petrophysical driven parameters except for S_w. The core derived Sw couldn't be validated with the log derived Sw because the core derived S_w was too low to be considered reliable. The shale reservoirs consist of clay which consists of bound water and the small sediment size is always related to higher irreducible water, so S_w of 0.03-0.09 can be taken as reliable outcome keeping in view the above constraints. For mitigating the S_w issue, all the parameters were matched with core parameter and log-derived qv was validated with the representative clay interval to calculate the Sw. It became inevitable to run the sensitivity analysis on the calculated Sw to check for the sensitivity of the input parameters. The whole results of the petrophysical campaign are tabulated in the (Tables 4-5). The tornado chart (Fig.17) shows the impact of the uncertainty of each variable used in the uncertainty analysis. The Tornado chart

shows that the largest impact on the water saturation (S_w) calculation is of Porosity of shale, bound water, m exponent and resistivity respectively. This further supports the idea of having core derived CEC to calculate S_w with better accuracy.

Conclusions

On the basis of porosity, permeability, TOC, S_w, mineral model and petrophysical model outcome, the Murteree Shale exhibits better potential basin-wide than the Roseneath Shale, which looks prospective in and near Encounter-01 well area in (Table. 3).

- Multiple mineral analysis yields better results than simple deterministic petrophysical analysis. The matching of input curves and output curves utility of multiple mineral analyses makes it a better choice to validate the model in surrounding of the analysed well.
- A mineral model can only be validated in an area if the XRD mineral analysis is present, which can be grouped according to a necessity to compute output. This can also be done by acquiring ECS logs but they still needs to be calibrated against a more direct measurement i.e. XRF and XRD.
- The Juhasz normalized Q_v approach can be used in the evaluation of shale gas reservoirs with considerable accuracy even when the reservoir consists of relatively fresh water. In fresh water formations the S_w estimation is very sensitive to bound water (Dual water model) and Q_v (Juhasz), so it need to validate these parameters to representative shales. It was done by correlating Q_v with representative shale (Fig. 14).
- On the basis of uncertainty analysis, caution is required to compute porosity of shale, bound water, m exponent and processing and environmental corrections of resistivity.
- The dean stark S_w was not useable because it was giving too low of values. It may be either due to cores were lying for years in a yard to extreme environmental conditions or that the cores were mishandled.
- PDP results show permeability of Roseneath and Murteree to be more sensitive to changes in confining pressure rather than pore pressure.

Future Considerations:

- To fully understand the shale gas potential of the basin there is an intense need to run Elemental Capture Spectroscopy (ECS), Nuclear Magnetic Resonance (NMR) and extensive coring along with conventional wireline logs. This would greatly enhance the core-to-log tie and would aid in understanding of the pore geometry of the shale gas reservoirs, subsequently helping in better understanding the shale gas reservoirs and their producibility. This study also demonstrates the importance of obtaining the Cation Exchange Capacity (CEC) from the core along with Archie exponents and capillary pressure data.

Acknowledgement

The Q.J would like to acknowledge funding provided by the Graduate Research Support Programmed for Ph.D. in the Department of Earth and Oceans Sciences at James Cook University. DMITRE (Department for Manufacturing, Innovation, Trade, Resources and Energy, Government of South Australia) generously provided core samples for this study. The authors are grateful for the technical services rendered by Synergy (IP Software), and Trican Geological Solutions Ltd, Calgary, Alberta, Canada, (XRD data). Special thanks are expressed to David Herrick for his critical review of the paper, Yellowstone Petrophysics, Wyoming, USA. We also acknowledge colleagues of sedimentology research group (Gravel Monkeys) at JCU, in particular Cassy Mtelela and Prince Owusu Agyemang. Q.J also acknowledges Fawahid Khan Jadoon (Comsat) and Tahir Khan (LMKR).

References

Archie, G.E. 1942. The electrical resistivity log as an aid in determining some reservoir characteristics. *Transactions of the American Institute of Mining and Metallurgical Engineers*, 146**,** 54–62.

Boucher, R.K., 2000. Analysis of seals of the Roseneath and Murteree Shales, Cooper Basin, South Australia. South Australian Department of Primary Industries and Resources. Report Book 2001/015.

Bust, V.K., Majid, A.A., O LETO, J.U & Worthington, P.F, 2011. The petrophysics of shale gas reservoirs; Challenges and pragmatic solutions (IPTC 14 631) In: international petroleum Technology conference, volume2, society of petroleum Enginees, Richson Tx.1440-1454.

Cluff, 2012, How to access shales from well logs, IOGA 66th Annual Meeting, Evansville, Indiana. Battersby, DG.,1977-Cooper Basin gas and oil fields.In:Leslie,R.B., Evans, H.J., & Knight,C.L.,(eds), Economic Geology of Australia and papua New Guinea, 3, Petroleum Australian Institute of Mining and Metallurgy, Parkville.

Chaney, A.J., et al., 1997, Reservoir Potential of Glacio-Fluvial Sandstones: Merrimelia Formation, Cooper Basin, S.A., APEA Journal v.37 p.154

Clavier, C., G., Coates, and J. Dumanoir, 1977, the theoretical and experimental bases for the dual-water model for the interpretation of shaly sands. SPE 6859, October.

Clavier, C., Coates, G. & Dumanoir, J. 1984. Theoretical and experimental bases for the dual-water model for interpretation of shaly sands.Soc. Pet. Eng. J. 24, 153–167.

Crain E. R., 2000, Crain's Petrophysical handbook, Access via: https://spec2000.net/11-vshtoc.htm.

Cui, X., A. M. M. Bustin, and R. M. Bustin, 2009, Measurements of gas permeability and diffusivity of tight reservoir rocks: Different approaches and their applications: Geofluids, v. 9, p. 208–223, doi: 10.1111/j.1468-8123.2009.00244.x.

DMITRE Resources and Energy Group, 2012. Coal deposits in South Australia. South Australia Earth Resources Information Sheet M23, February 2012. Access via: https:// sarigbasis.pir.sa.gov.au/WebtopEw/ws/ samref/sarig1/image/DDD/ISM23.pdf.

Daniel A. Krygowski, 2003. Austin Texas USA: Guide to petrophysical interpretation, DEN5 pp. 47.

Gatehouse, C.G., 1972-Formations of the Gidgealpa Group in the Cooper Basin. Australasian Oil & Gas Review 18:12, 10-15.

Glorioso, J.C and A.J Rattia (2012). "Unconventional Reservoirs: Basic petrophysical concepts for shale Gas "SPE/EAGE European Unconventional Resources conference and Exhibition Vienna, Australia, Society of Petroleum Engineers.

Gravestock, D.I. and Flint, R.B., 1995. Post-Delamerian compressive deformation. In: Drexel, J.F. and Preiss, W.V.

Gravestock, D.I., 1998. Cooper Basin: Stratigraphic frameworks for correlation. In: Gravestock, D.I., Hibburt, J.E. and Drexel, J.F. (Eds.) the Petroleum Geology of South Australia. Volume 4, Primary Industries and Resources South Australia, Report Book 98/9, pp. 117–128.

Guidry, D.L. Luffel, 1990, Devonian Shale Formation evaluation model based on logs, new core analysis methods, and production tests. P.n 6.

Herrick, D.C., and Kennedy, W.D., 1994, Electrical efficiency. A pore geometric theory for interpreting the electrical properties of reservoir rock: Geophysics, V.59, pp. 918-927.

Hill, A.J., 1995. Source rock distribution and maturity modelling. In: Morton, J.G.G. and Drexel, J.F. (Eds), the petroleum geology of South Australia. Volume 1: Otway Basin. South Australia. Department of Mines and Energy Report Book, 95/12:103-125.

Kathy R. Bruner and Richard Smosna, A comparative study of the Mississipian Barnet Shale, Fort Worth Basin, and Appalachian Basin, 2011, pp 5-70.

Jadoon, Q.K., Roberts. E., Blenkinsop,T., Wüst, R.A.J., Shah,A Mineralogical modelling and petrophysical parameters in Permian gas shales from the Roseneath and Murteree formations, Cooper Basin, Australia (In press).Petroleum Exploration and Development(March 2016).

Jadoon, Q.K., Roberts. E., Blenkinsop,T., Wüst, R.A.J Organic petrography and thermal maturity of the Permian Roseneath and Murteree shales in the Cooper Basin, Australia, Int.J.Coal Geol.(2016), http://dx.doi.org/10.1016/j.coal.2016.01.005

Juan C. Glorioso, Asquile Rattia, Repsol, Unconventional Reservoir: Basic Petrophysical Concepts for Shale Gas, pp 1-8.

Juhaz, I.(1981) Normalized Qv-the key to shaly sand evaluation using the Waxman-smits equation in the absence of core data.In Transactions of the SPWLA 22nd annual logging symposium, society of professional wel log analysis, Houston, TX, pp, 21-36.

Kapel, A.J., 1972. The geology of the Patchawarra area, Cooper Basin. APEA Journal, 6:71-7.

Kathy, R, Brumen and Richard Smosna, 2011. A comparative study of the Mississpian Barnett Shale, Fort Worth Basin, and Devonian Marcellus Shale, Applachian Basin, US Department of Energy, DDE/NEIL-2011/1478.

Keller, A. and J.Bird, 1999 , The oil and Gas Resource Potential of the 1002 Area, Arctic National Wildlife Refuge, Alaska, by ANWR assessment Team, U.S> Geological Survey Open File Report 98-34.troleum source rock Evaluation. The oil and Gas resources potential Alaska.

Klemme, H.D., 1980 - Petroleum basins- classifications and characteristics. Journal of petroleum geology vol.3, pp. 187-(Abundance & Lindsay, 2000).

Kowalczyk, P., S. Furmaniak, P. A. Gauden, and A. P. Terzyk, 2010, Carbon dioxide adsorption-induced deformation of microporous carbons: Journal of Physical Chemistry C,v. 114, p. 5126–5133, doi:10.1021/jp911996h

Krygouski, D. 2003. Guide to petrophysical interpretation.

Melissa Vallee, 2013, Petrophysical Evaluation of Lacustrine Shales in the Cooper Basin, Australia. Pp. 1

Myers, R. (2008). Marcellus shale update, Independent Oil & Gas Association of West Virginia.

Passey, O.R., Mor etti, F.U., Stroud, J.D., 1990, A practical modal for organic richness from porosity and resistivity logs. AAPG Bulletin 74, 1777–1794.

Passey QR, Bohacs KM, Esch WL, Klimentidis R, Sinha S(2010) From oil- prone source rock to gas-producing shale reservoir-Geologic and petrophysical characterization of unconventional shale-gas reservoirs,SPE 131350.

Peters, K.E., 1986 – Guidelines for evaluating petroleum source rocks using programmed pyrolysis. American Association of Petroleum Geologist Bulletin 70, pp.318-30.

Peters, K.E., Moldowan, J.M., 1993. The Biomarker Guide: Interpreting Molecular Fossils in Petroleum and Ancient Sediments. Prenctile-Hall, Englewood Cliffs, NJ.

Peters, K. E., Walters, C. C., Moldowan, J. M. The Biomarker Guide. Vol. 2: Biomarkers and Isotopes in Petroleum Exploration and Earth History. 2rd ed – Cambridge, 2004. pp. 475–1155.

PIRSA, 2000 www.pir.sa.gov.au/__data/assets/pdf_file/0019/27226/cooper_prospectivity.pdf.

PIRSA (Primary Industries and Regions of South Australia), 2007 Petroleum Geology of South Australia, Volume 4: Cooper Basin. South Australian Department of Primary Industries and Resources. Report Book 203-09

Price, P.L., Filatoff, J., Williams, A>J., Pickering, S.A., & Wood, G.R., 1985- Late Paleozoic and Mesozoic palynostratigraphic units, CSR Ltd: Oil & Gas Division. Unpublished company report 274/25.

Ramirez, T. R., Klien, J. D., Bonnie, R.J.M. & Howard, J.J. 2011. Comparative study of formation evaluation methods for unconventional shale-gas reservoirs: application to the Haynesville Shale (Texas). SPE paper 144062, Society of petroleum engineer, Richardson, Texas.

Stuart, W.J., 1976. The genesis of Permian and Lower Triassic reservoir sandstones during phases of southern Cooper Basin.

Tissot, B.P., Welte, D.H., 1984. Petroleum Formation and Occurrence, second ed. Springer-Verlag. Berlin, 699p.Juhasz, I., 1981, Normalized Qv – the key to shaly sand elaluation using the Waxman-Smits equation in the absence of core data, Transactions, SPLWA 22nd Annual Logging Symposium, June 23-26, paper Z.

Vivian K. Bust, Azlan A. Majid, 2011. The Petrophysics of Shale Gas Reservoirs: Technical Challenges and Pragmatic Solution. Pp 2-4

Abundance, A. M., & Lindsay, J. (2000). Source Rock Potential and Cooper Basin , South Australia, (September).

W. David Kennedy and David C. Herrick, 2012, Geophysics, volume 77, No.3. Conduction models of Archie rocks, pp. 2.

Waxman, M. H., and Smits L. J. M., 1968, Electrical conductivities in oil-bearing sands, SPE Journal, June pp. 107-122.

Waxman, M.H. and Thomas, E.C. (1974) Electrical conductivities in the shaly sands. I. The relation between hydrocarbon saturation and resistivity index; II. The temperature coefficient of electrical conductivity SPE Journal, February.

Williams, P.F.V., and A.G. Douglas., 1983. A preliminary organic chemistry investigation of the Kimmeridgian oil shales. In A.G. Douglas and J.R. Maxwell (eds.), Advances in organic geochemistry 1979, Oxford: Pergamon Press, pp.531-545.

Williams, B.P.J., Wild, E.K., & Suttill, R.J., 1985-Paraglacial aeolianites: Potential new hydrocarbon reservoirs, Gidgealpa Group, southern Cooper Basin.The APEA journal 25:1, pp. 291-310.F.K. Worthington, P.F. 2011a. The petrophysics of problematic reservoirs. Journal of Petroleum Technology 63(4), 261-274.

Wopfner, H., 1972-Depositional history and tectonics of South Australian sedimentary basins. South Australian Mineral Resources Review 113, 32-50.

Worthington, P.F. 2011*a*. The petrophysics of problematic reservoirs. Journal of Petroleum Technology, **63**, (12), 88–97.

Worthington, P.F. 2011*b*. The direction of petrophysics – a perspective to 2020. *Petrophysics*, **52**, 261–274.

Wüst, R.A.J., Hill., Jadoon, Q.k., Nassichuk, and Alexander, 2015, Permian Lacustrine Unconventional Shales as Hyrocarbon Targets in the Cooper Basin, Australia: Rock Characteristics and Well and Production Challenges Feb 2015(Applied Geoscience Conference-Houston Geological Society (USA).

www.issuu.com/thepick/docs/**pesa**_133_forweb.PetroleumExploration Society of Australia (PESA), 2014.

Figure 1: Map of study area, star symbols showing cored wells and blue dots showing well locations in the Cooper Basin, Australia (modified after Chaney et al., 1997).

Figure 2: Stratigraphy of the Cooper Basin (PIRSA, 2007). Arrow shows the study interval that includes the Roseneath and Murteree shales. PIRSA 200171_2 and 200171_004.

Figure 3: Comparison of petrophysical model and core data from the Roseneath Shale of the Encounter-1 well: gamma ray (GR), resistivity (M2RX, M2R2), Density (RHOB), neutron (PHIN) and sonic (DT) logs. Mineralogical model demonstrating composition of clays, Illite - arylide yellow, kaolinite -olive green, siderite- blue shading, quartz- yellow, and kerogen with black colour. Red dots represent XRD core data. Volume of silt and clay is depicted in Track 15 and Track 16 shows log derived permeability matched with core derived permeability depicted by red dots.

Figure 4: Comparison of petrophysical model and core data from the Murteree Shale of the Ashbay-1 well: Gamma ray (GR), resistivity (LLD, LLS, and MSFL), Density (RHOB), neutron (PHIN) and sonic (DT) logs. Mineralogical model demonstrating composition of illite in arylide yellow , Kaolinite -olive green, siderite- blue shading, quartz- yellow, and kerogen with black colour. Red dots represent XRD core data and porosity and permeability. Volume of silt and clay are depicted in Track 16 while Track 17 shows comparison of log derived permeability with core derived permeability.

Figure 5: Comparison of petrophysical model and core data from the Murteree Shale of the Dirkala-02 well: Track-1 to 16. Track-1: gamma ray (GR), Track-3: Resistivity (RESS, RESM, RESD), Track-4: Caliper (CALI). Track-05: Density (RHOB), Neutron (NPHI) and sonic (DT), Track 12: Estimation of Porosity, In Track 13: Mineralogical model demonstrating composition of illite in arylide yellow colour, Kaolinite -olive green, siderite- blue shading, quartz- yellow, and kerogen with black colour. Red dots represent XRD core data, Track15: volume of silt and clay, Track 16: Shows permeability.

Figure 6: Comparison of well log interpretation and core data for Moomba-73 well, Murteree shale section: Track1: gamma ray (GR), Track4: Resistivity (LLS, LLD), Track5: Caliper (CALI), Track6: Sonic (DT) Track9: Estimation of Porosity, Mineralogical model demonstrating composition of clay in green colour, quartz- yellow, and kerogen with black colour. Track 12: showing match between input and model generated sonic curve, Track 13: showing match between input and model generated Gamma ray curve, Track 14: Shows log derived permeability.

Figure 7: Mineral model for the Murteree Shale in Dirkala-01 well. No core data was present for this well so the output parameters of Dirkala-02 were used as input for this well. Track 8: mineralogical model demonstrating composition of illite in grey colour, kaolinite -olive green, siderite- bright green shading, quartz- yellow, and kerogen with black colour.

Figure 8: Corss-plot between permeability and total confining pressure: Permeability points were selected for true effective stress values of 18, 39, and 62 MPa to get a relationship between the permeability and total confining stress. It was later used to remove the overburden effects. The sample represents a depth of 3387.39 of Encounter-01 well.

Figure 9: Corss-plot between permeability and total confining pressure: Permeability points were selected for true effective stress values of 9, 23, and 33 MPa to get a relationship between the permeability and total confining stress. It was later used to remove the overburden effects. The sample represents a depth of 1892.8 of Dirkala-02 well.

Figure 10: Corss-plot between permeability and total confining pressure: Permeability points were selected for true effective stress values of 15, 32, and 45 MPa to get a relationship between the permeability and total confining stress. It was later used to remove the overburden effects from core permeability. The sample represents a depth of 2080.11 of Ashbay-01 well.

Figure 11: Permeability versus depth plot of samples from 5 different wells Encounter-1, Tirrawarra-1, Dirkala-2, Big Lake 48(South Australia) Ashby-1 and Epsilon (Queensland area) Permeability is in range of milidarcy md in all wells except Tirrawara-2 and Epsilon-2.

Figure 12: Picket plot of resistivity (Ohm.m) against total porosity (V/V) for Ashbay-01 well showing a classical example to find R_w in water zone. The linear trend at the south west of the cluster represents a water wet zone and Ro line was set at its base. An R_w of 0.5 was computed. Picket plot being graphical representation of Archie equation shows wet point in linear form.

Figure 13: Picket plot of resistivity (ohm.m) versus total porosity (V/V) a threshold of 0.25 was set in order to take R_{wb} in the shaly part of the formation. R_{wb} of 0.11 was computed.

Figure 14: Cross plot between the PHIT and App Qv, a linear relationship can be seen in green water wet interval. Waxman and Smit's 'a' and 'b' are determined by this cross-plot. The blue circle shows area of Glauconite and red circle shows area of Orthoclase. Both the circles are situated at higher Qv value suggesting that both the minerals have Qv higher than other clay minerals. Since the log derived Qv should be correlated to an appropriate porosity measurement in order to define a Qv –ϕT relationship, either in the form of Qv = a ϕT ^-b Or Qv = a/ϕT –b. The obtained relationship is then applied to the hydrocarbon bearing section to calculate Qv.

Figure 15: Kerogen embedded in a clay-rich matrix with low porosity in the Murteree Shale in Dirkala-2 well. Open pores measure from 10-50 nm to ~ 2 µm. Some authigenic quartz coatings are observed (Jadoon et al., 2016)

Figure 16: Photomicrograph of an organic rich shale in Murteree Dirkala-2 showing well-opaque organic material nearly 2mm wide. Cross Polarized light (60X).

Figure 17: shows the impact of the uncertainty of each variable used in the uncertainty analysis. The Tornado chart show that that the largest impact on the water saturation (Sw) calculation is of Porosity of shale and bound water resistivity, followed by m exponent and resistivity respectively. This further supports the idea of getting special core analysis (SCAL) to determine core derived CEC, electrical properties (a,m & n) to calculate Sw with better accuracy.

Table.1: Showing use of core and log data (modified after Cluff, 2012)

Property of Interest	Core data	Log data
Porosity	Crushed dry rock He porosimetry	Density (mostly)
TOC	Rock Eval	GR, density, resistivity
Water saturation	As- received retort or Dean-Stark	Resistivity +kerogen corrected porosity
Mineralogy	XRD, SEM, Thin section, ICPMS	Density, neutron, PE, ECS-type logs
Permeability	Pulse decay Permeability	Core plugs
Geomechanics	Static moduli	DTC,DTS,RHOB, & Synthetic substitutes
Geochemistry	R_0, S1-S2-S3, etc.	Resistivity

Table.2: Showing the methodology for Petrophysical analysis, modified after (Bust et al., 2011)

Key wells		**Non- key wells**
TOC Determination		**TOC Determination**
Core-TOC measurement (Rock-Eval Pyrolysis/Leco TOC) Log standard logs (density, spectral GR, resistivity, sonic). Log-standard logs (density, spectral, GR, resistivity, sonic)	Log VS TOC relationship →	Log- standard logs (density, spectral GR, resistivity, sonic).

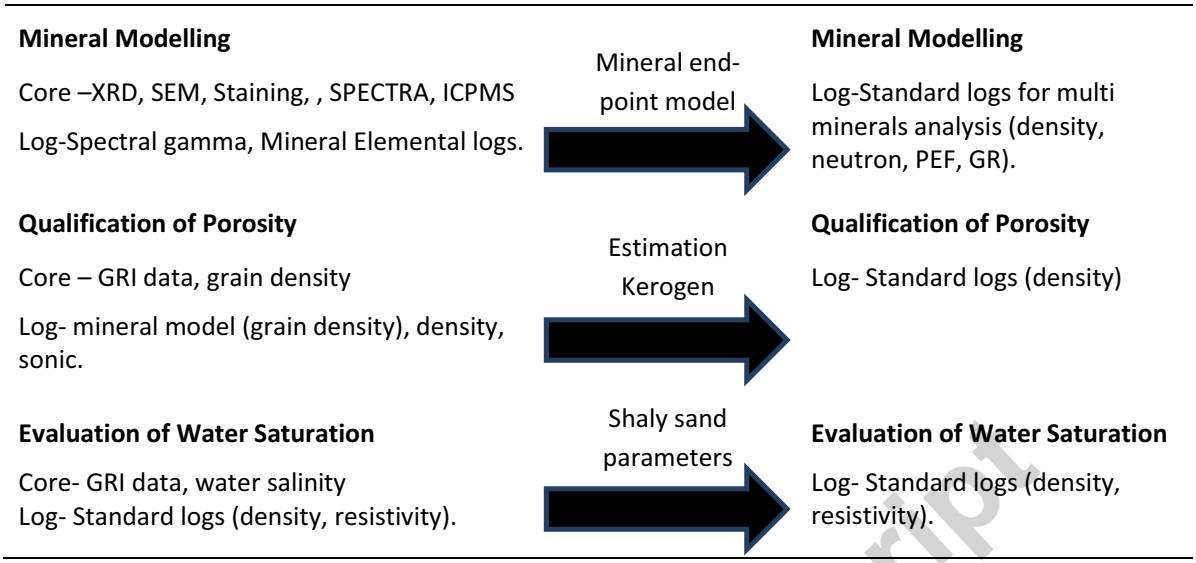

Table 3: Roseneath, Murteree Shale Shows key information of porosity, VCL, TOC, S_w and permeability**.**

Well name	Shale	Avg Phi%	Avg Sw%	Avg VCL%	Avg TOC wt %	Permeability nd
Dirkala-1	Roseneath	2	100	50	1.5	$5.5 * 10^{-5}$
Baratta-2	Roseneath	4	90	75	1	-
Ashbay-1	Roseneath	4	76	48	1.5	-
Moomba-73	Roseneath	2	63	47	4	$5.1 * 10^{-5}$
Toolache-N-1	Roseneath	5	70	53	2.6	-
Moomba-66	Roseneath	4	60	50	3	$6 * 10^{-5}$
Toolache-39	Roseneath	5	90	55	1.8	-
Big Lake-70	Roseneath	3.5	-	80	-	$4.5 * 10^{-6}$
Della-1	Roseneath	1.5	95	58	0.9	-
Dirkala-2	Roseneath	3	90	60	1	$3 * 10^{-5}$
Encounter-1	Murteree	4.5	60	60	3.5	$1.5 * 10^{-5}$
Dirkala-1	Murteree	10.2	60	52.1	1.6	$3.5 * 10^{-5}$
Barata-02	Murteree	3.5	85	70	1.1	-
Ashbay-01	Murteree	3.6	65	41	1.4	$5.1 * 10^{-5}$
Moomba-73	Murteree	8	59	55	4.1	$4.1 * 10^{-5}$
Toolache-N-1	Murteree	4.8	50	54	3.3	-
Moomba-66	Murteree	4.4	62	49	3.3	$3.5 * 10^{-5}$
Toolache-39	Murteree	6	79	50	2.5	-

Big Lake-70	Murteree	3.2	-	75	-	$4.14 * 10^{-6}$
Della-01	Murteree	4.1	55	55	2.1	-
Dirkala-02	Murteree	10	48	48	1.6	$3.8 * 10^{-5}$
Encounter	Murteree	6	55	57	2.2	$1.92 * 10^{-5}$

Highlights

- Format the whole paper is changed according to the reviewers
- Paper name is modified
- Delete some unrelated information in the Geological Setting part.
- Changed the map and stratigraphy section
- Add the Pulse decay data and Figs (Permeability derived from core plugs and match with Petrophysical models).
- Improved the Petrophysical models and mineral model with kerogen precisely rather than TOC and add the permeability track in the model and tie up with core. Add the more tracks in the models.

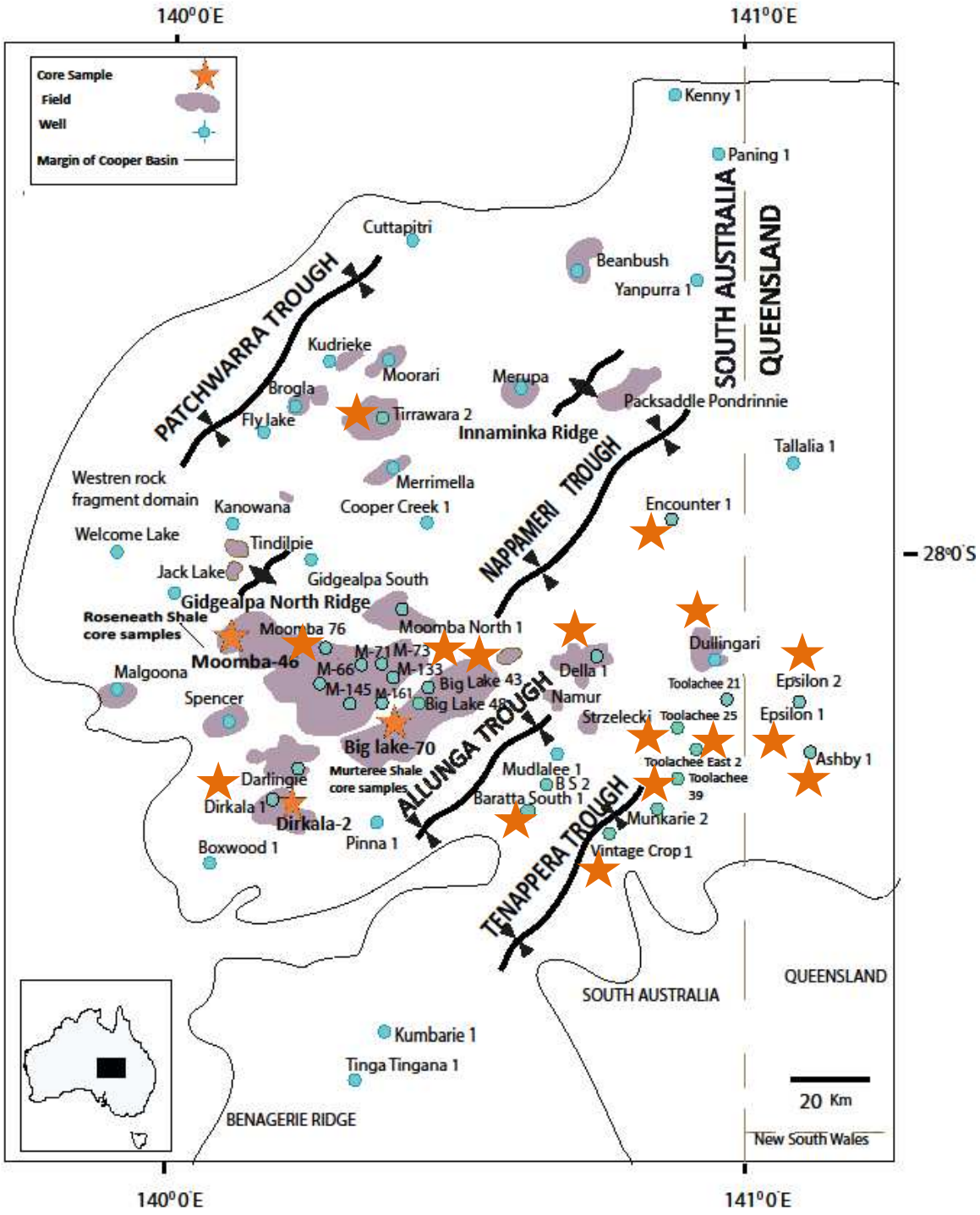

Figure 1: Map of study area, star symbols showing cored wells and blue dots showing well locations in the Cooper Basin, Australia (modified after Chaney et al., 1997).

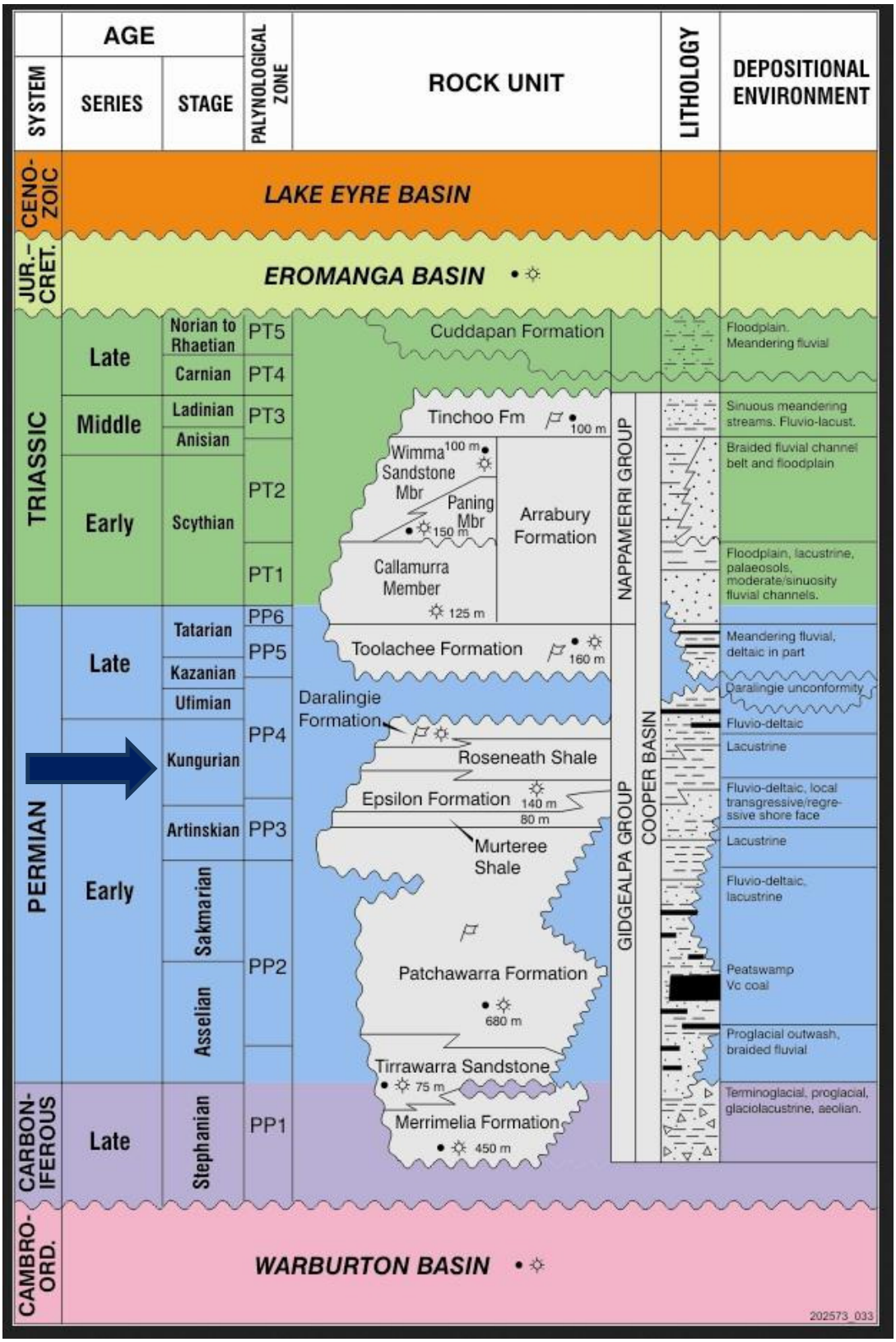

Figure 2: Stratigraphy of the Cooper Basin (PIRSA, 2007). Arrow shows the study interval that includes the Roseneath and Murteree shales. PIRSA 200171_2 and 200171_004.

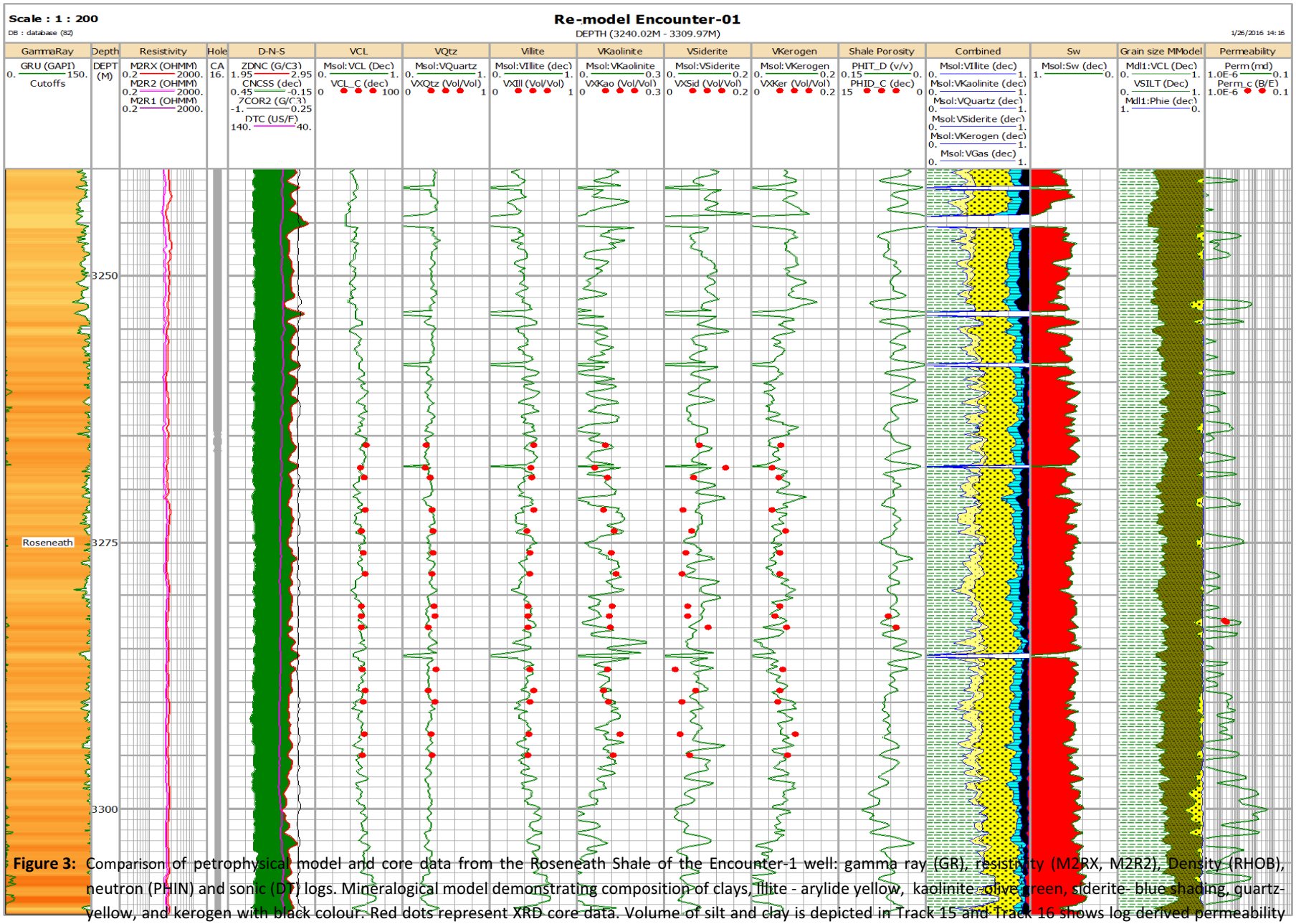

Figure 3: Comparison of petrophysical model and core data from the Roseneath Shale of the Encounter-1 well: gamma ray (GR), resistivity (M2RX, M2R2), Density (RHOB), neutron (PHIN) and sonic (DT) logs. Mineralogical model demonstrating composition of clays, Illite - arylide yellow, kaolinite -olive green, siderite- blue shading, quartz- yellow, and kerogen with black colour. Red dots represent XRD core data. Volume of silt and clay is depicted in Track 15 and Track 16 shows log derived permeability matched with core derived permeability depicted by red dots.

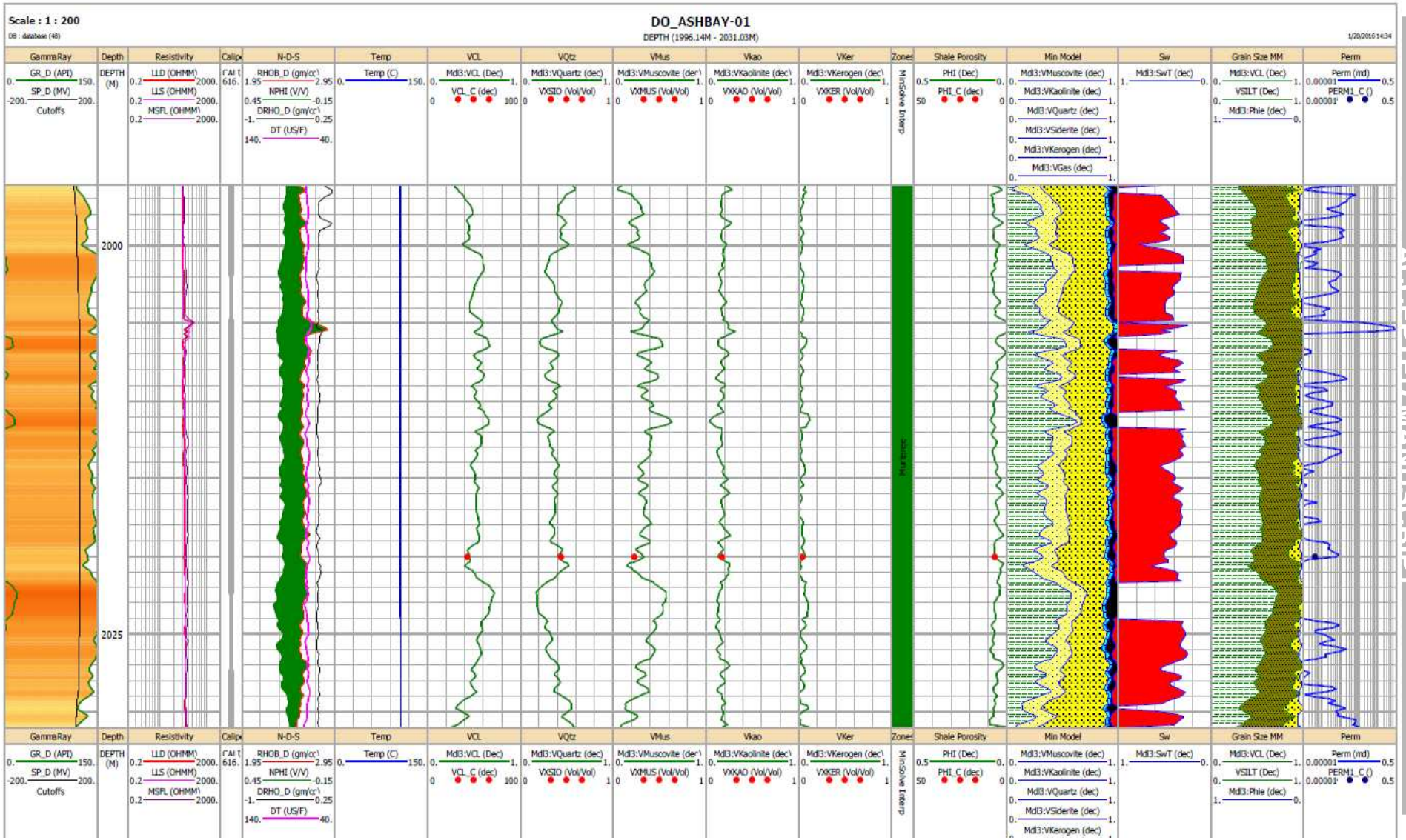

Figure 4: Comparison of petrophysical model and core data from the Murteree Shale of the Ashbay-1 well: Gamma ray (GR), resistivity (LLD, LLS, and MSFL), Density (RHOB), neutron (PHIN) and sonic (DT) logs. Mineralogical model demonstrating composition of illite in arylide yellow , Kaolinite -olive green, siderite- blue shading, quartz- yellow, and kerogen with black colour. Red dots represent XRD core data and porosity and permeability. Volume of silt and clay are depicted in Track 16 while Track 17 shows comparison of log derived permeability with core derived permeability.

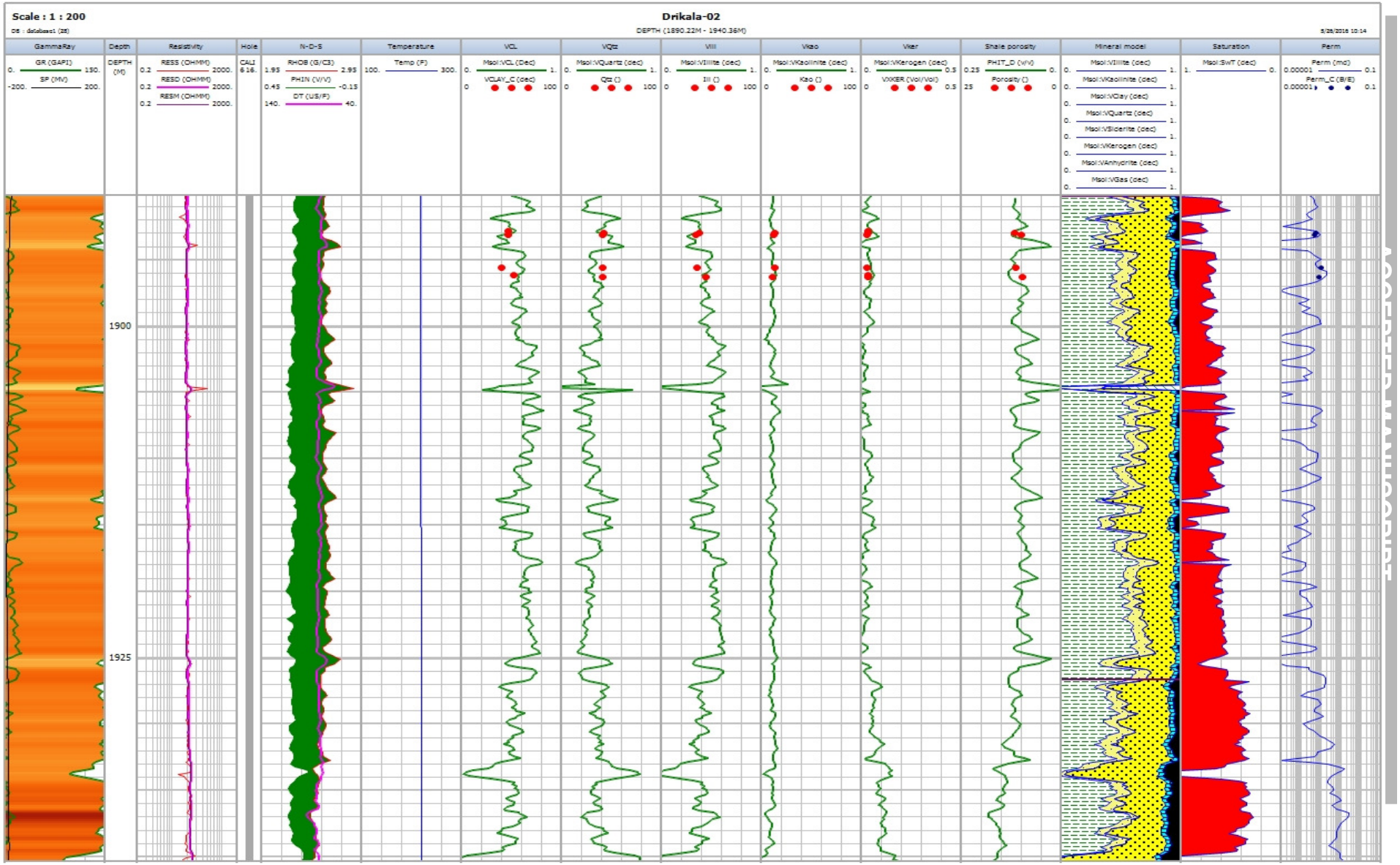

Figure 5: Comparison of petrophysical model and core data from the Murteree Shale of the Dirkala-02 well: Track-1 to 16. Track-1: gamma ray (GR), Track-3: Resistivity (RESS, RESM, RESD), Track-4: Caliper (CALI). Track-05: Density (RHOB), Neutron (NPHI) and sonic (DT), Track 12: Estimation of Porosity, In Track 13: Mineralogical model demonstrating composition of illite in arylide yellow colour, Kaolinite -olive green, siderite- blue shading, quartz- yellow, and kerogen with black colour. Red dots represent XRD core data, Track15: volume of silt and clay. Track 16: Shows permeability.

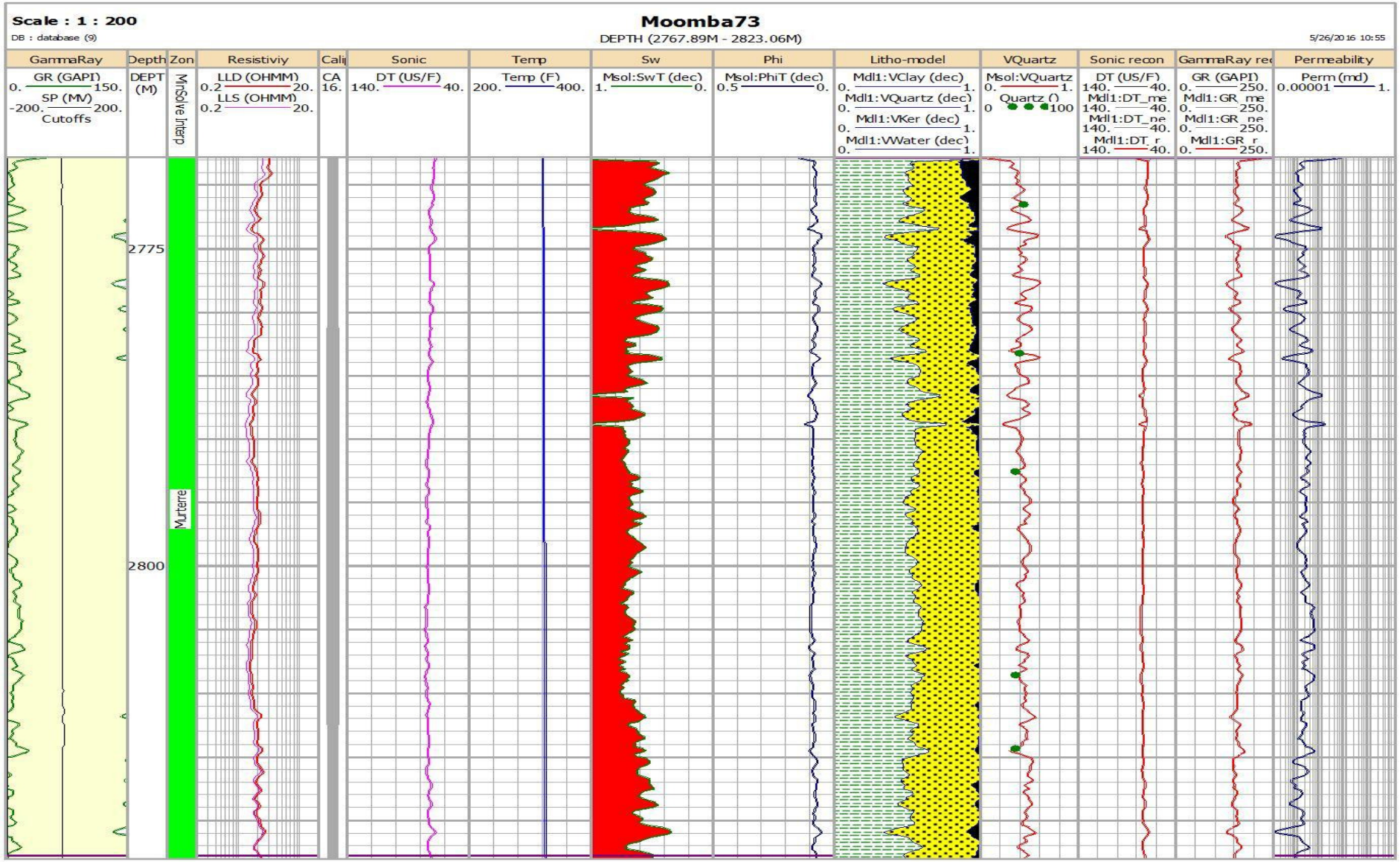

Figure 6: Comparison of well log interpretation and core data for Moomba-73 well, Murteree shale section: Track1: gamma ray (GR), Track4: Resistivity (LLS, LLD), Track5: Caliper (CALI), Track6: Sonic (DT) Track9: Estimation of Porosity, Mineralogical model demonstrating composition of clay in green colour, quartz- yellow, and kerogen with black colour. Track 12: showing match between input and model generated sonic curve, Track 13: showing match between input and model generated Gamma ray curve, Track 14: Shows log derived permeability.

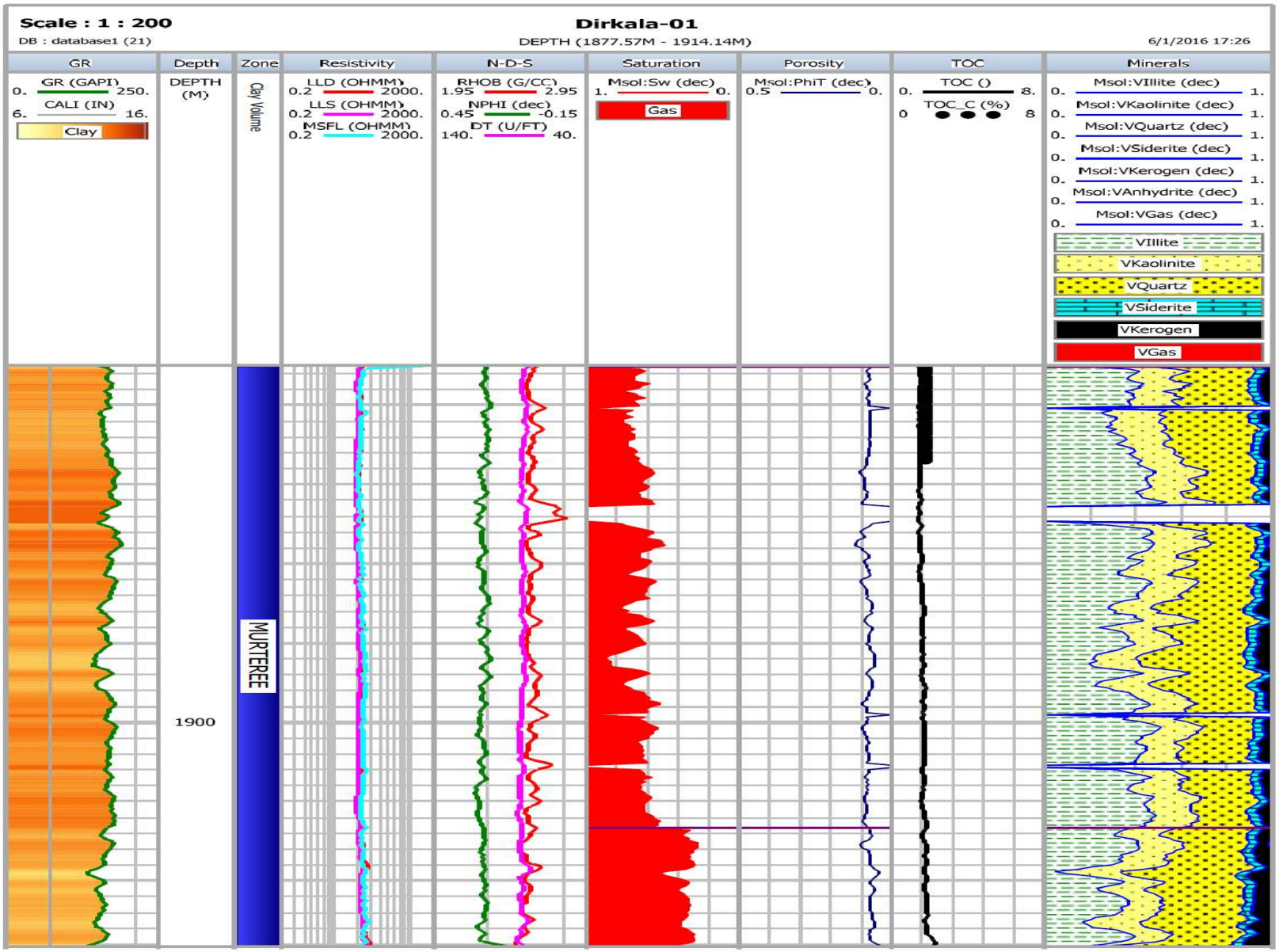

Figure 7: Mineral model for the Murteree Shale in Dirkala-01 well. No core data was present for this well so the output parameters of Dirkala-02 were used as input for this well. Track 8: mineralogical model demonstrating composition of illite in grey colour, kaolinite -olive green, siderite- bright green shading, quartz- yellow, and kerogen with black colour.

Well Name: Encounter-1 Sample depth: 3387.39 m

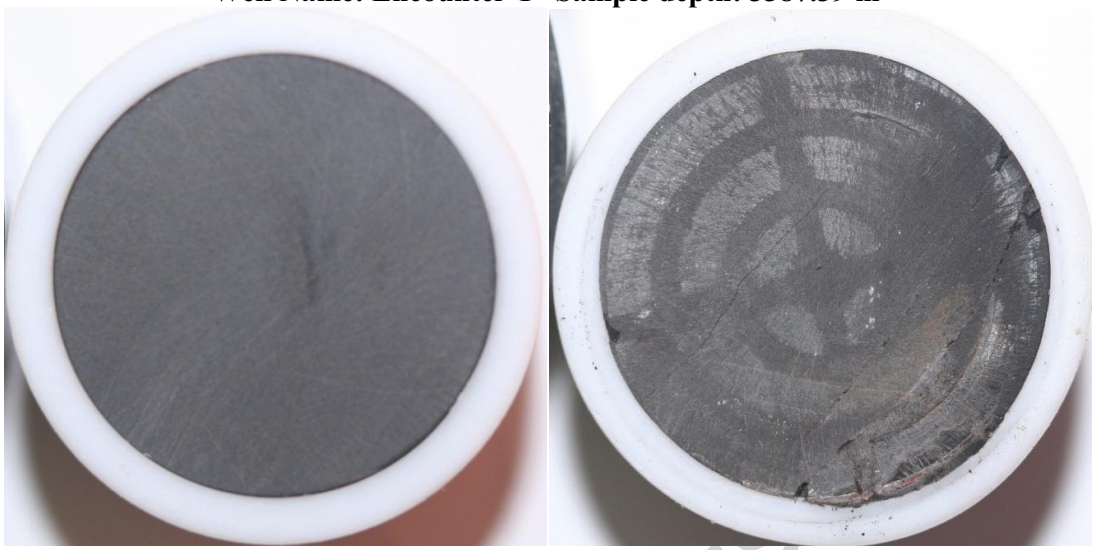

Before Assembly into Apparatus After Pulse Decay Test

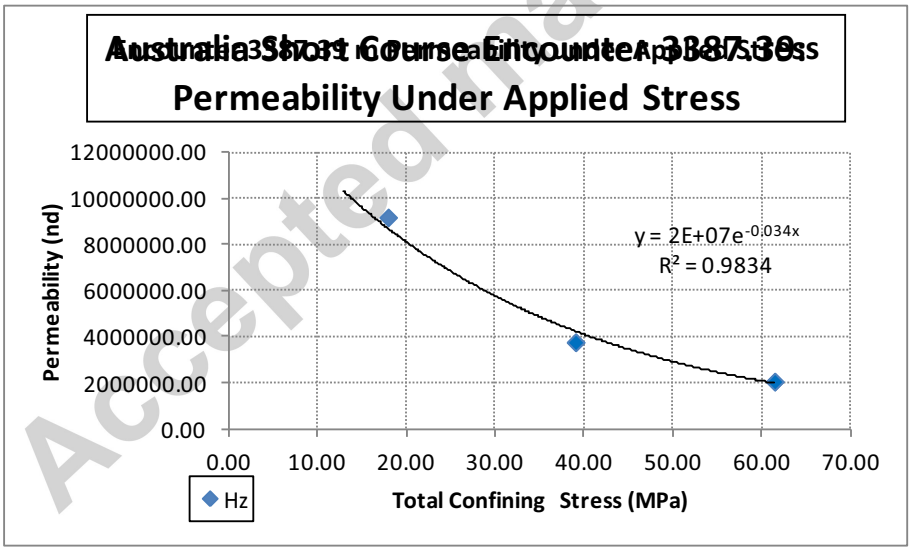

Figure 8: Corss-plot between permeability and total confining pressure: Permeability points were selected for true effective stress values of 18, 39, and 62 MPa to get a relationship between the permeability and total confining stress. It was later used to remove the overburden effects. The sample represents a depth of 3387.39 of Encounter-01 well.

Well name: Dirkala-2 Sample depth: 1892.88 m

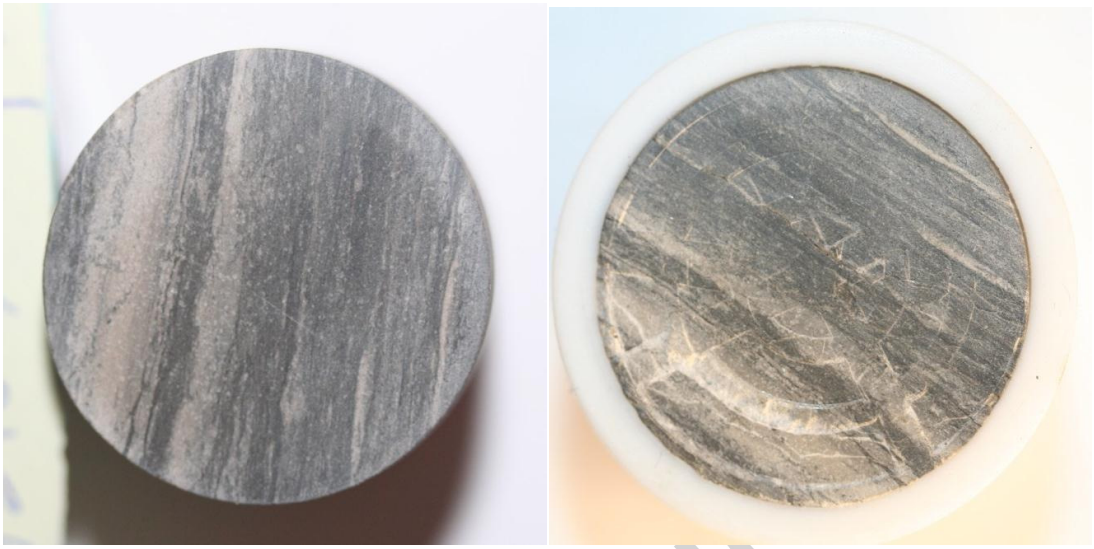

Before Assembly into Apparatus

After Pulse Decay Test

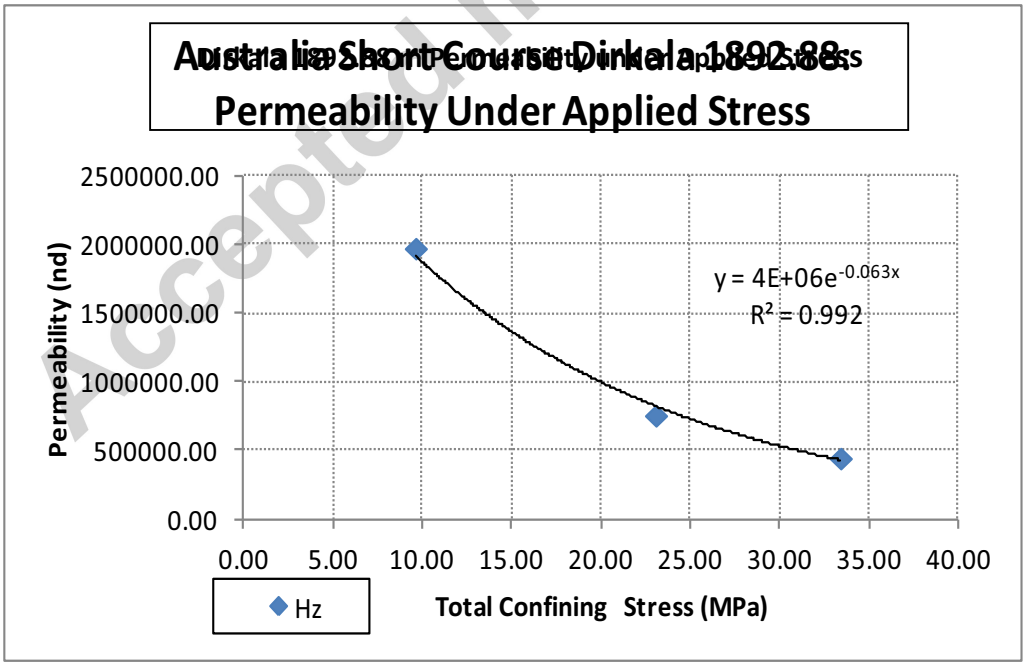

Figure 9: Corss-plot between permeability and total confining pressure: Permeability points were selected for true effective stress values of 9, 23, and 33 MPa to get a relationship between the permeability and total confining stress. It was later used to remove the overburden effects. The sample represents a depth of 1892.8 of Dirkala-02 well.

Well Name: Ashby-1 Sample depth: 2080.11 m

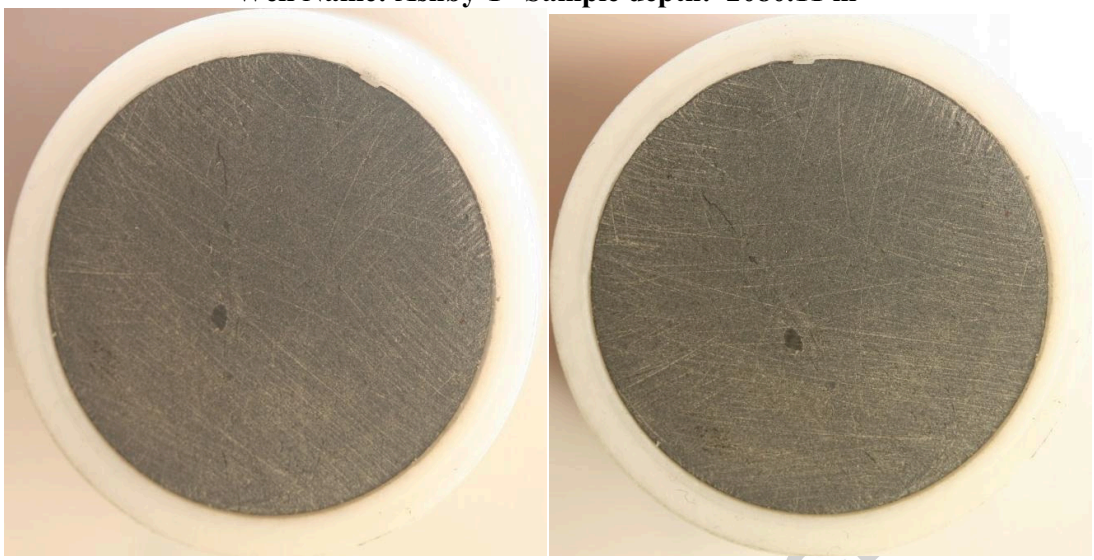

Before Assembly into Apparatus After Pulse Decay Test

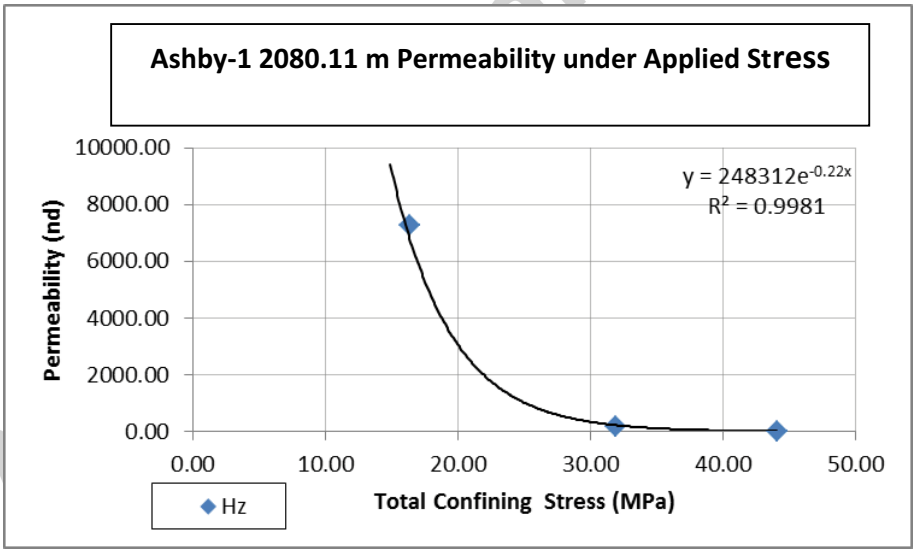

Figure 10: Corss-plot between permeability and total confining pressure: Permeability points were selected for true effective stress values of 15, 32, and 45 MPa to get a relationship between the permeability and total confining stress. It was later used to remove the overburden effects from core permeability. The sample represents a depth of 2080.11 of Ashbay-01 well.

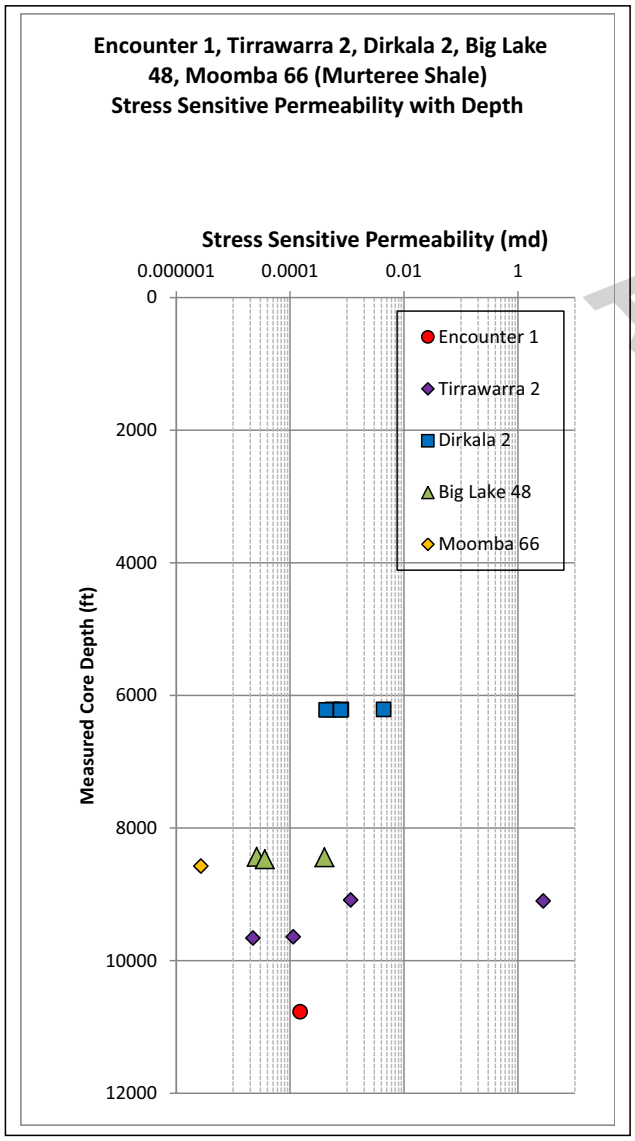

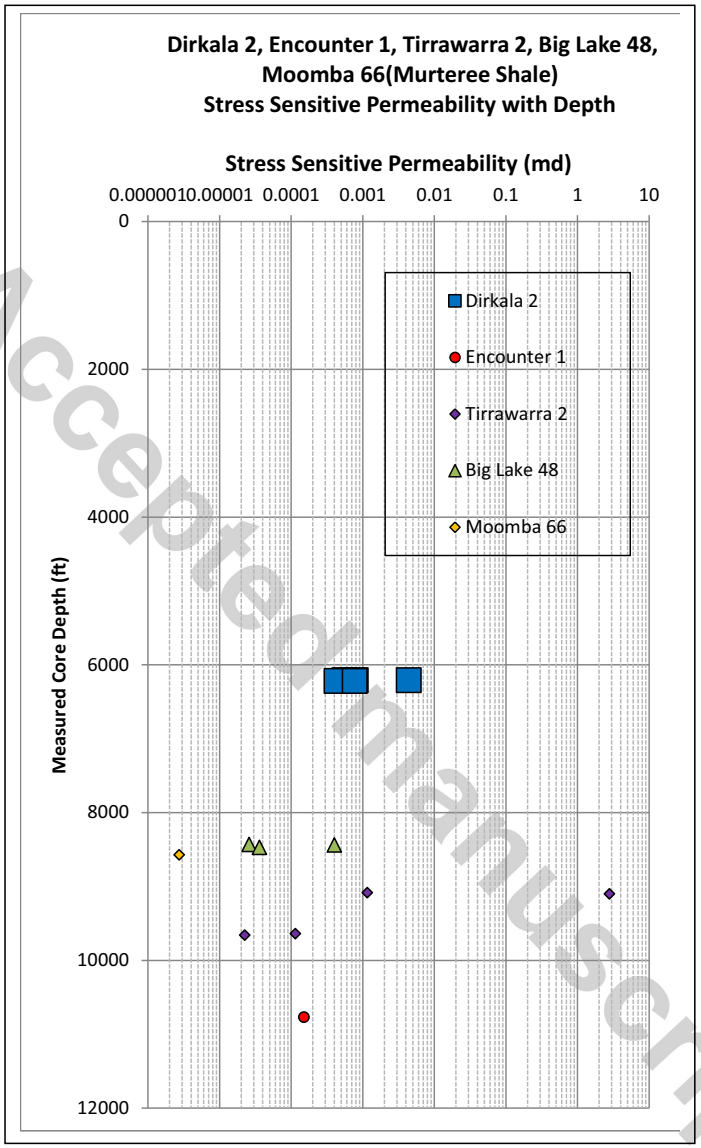

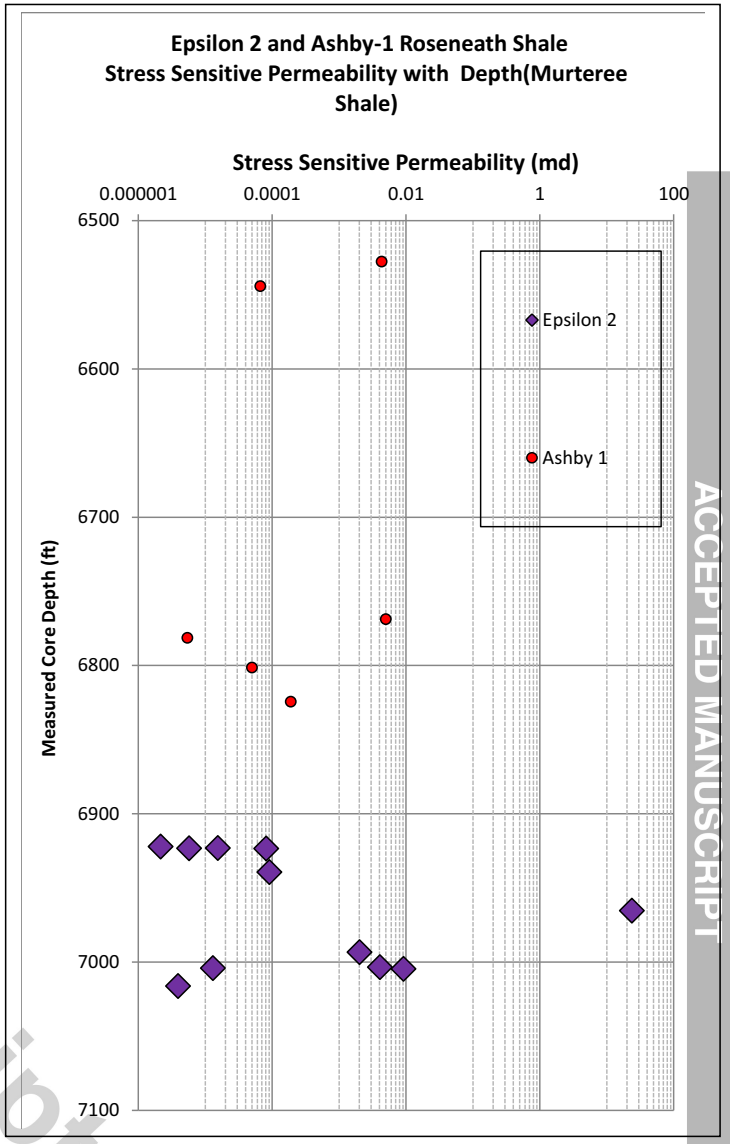

Figure 11: Permeability versus depth plot of samples from 5 different wells Encounter-1, Tirrawarra-1, Dirkala-2, Big Lake 48(South Australia) Ashby-1 and Epsilon (Queensland area) Permeability is in range of milidarcy md

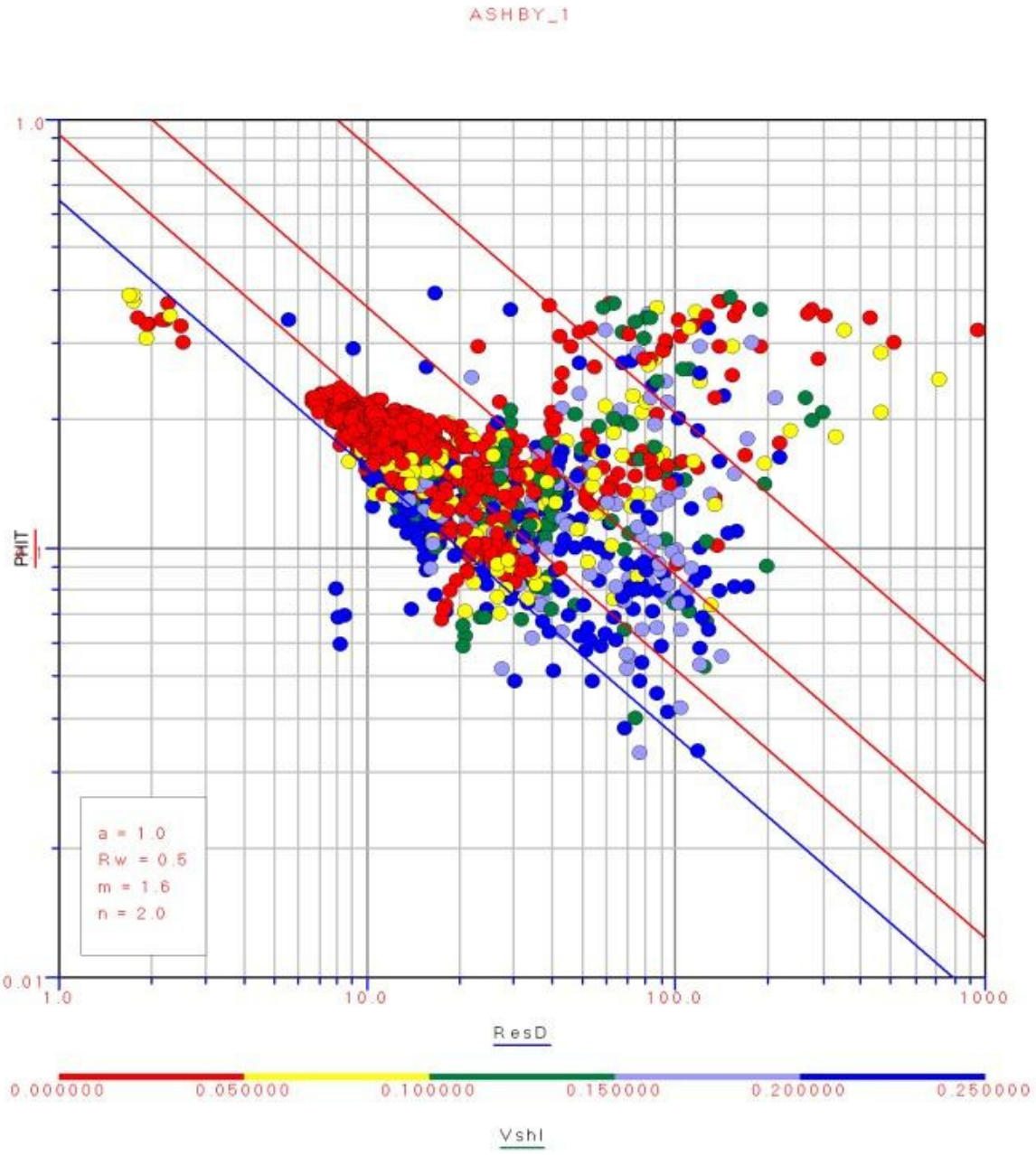

Figure 12: Picket plot of resistivity (Ohm.m) against total porosity (V/V) for Ashbay-01 well showing a classical example to find R_w in water zone. The linear trend at the south west of the cluster represents a water wet zone and Ro line was set at its base. An R_w of 0.5 was computed. Picket plot being graphical representation of Archie equation shows wet point in linear form.

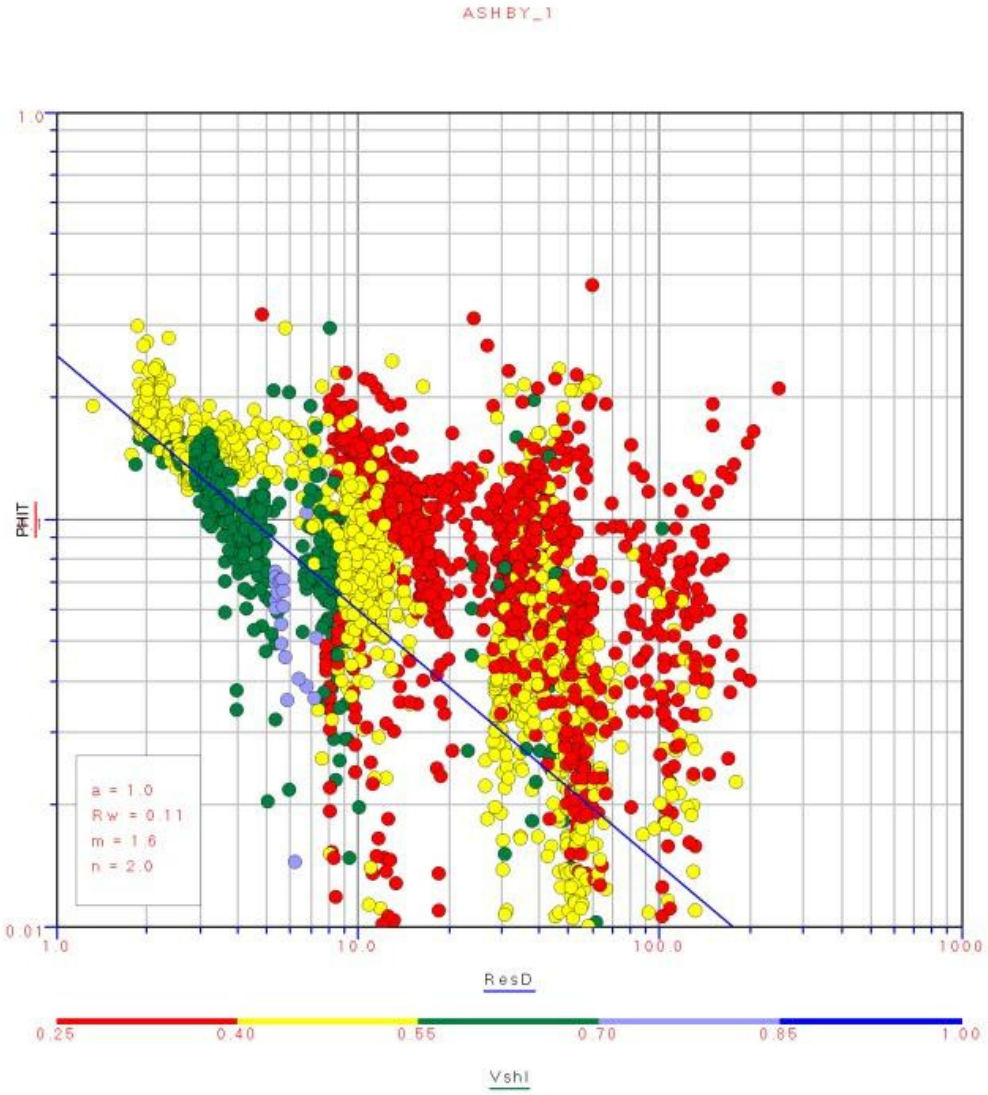

Figure 13: Picket plot of resistivity (ohm.m) versus total porosity (V/V) a threshold of 0.25 was set in order to take R_{wb} in the shaly part of the formation. R_{wb} of 0.11 was computed.

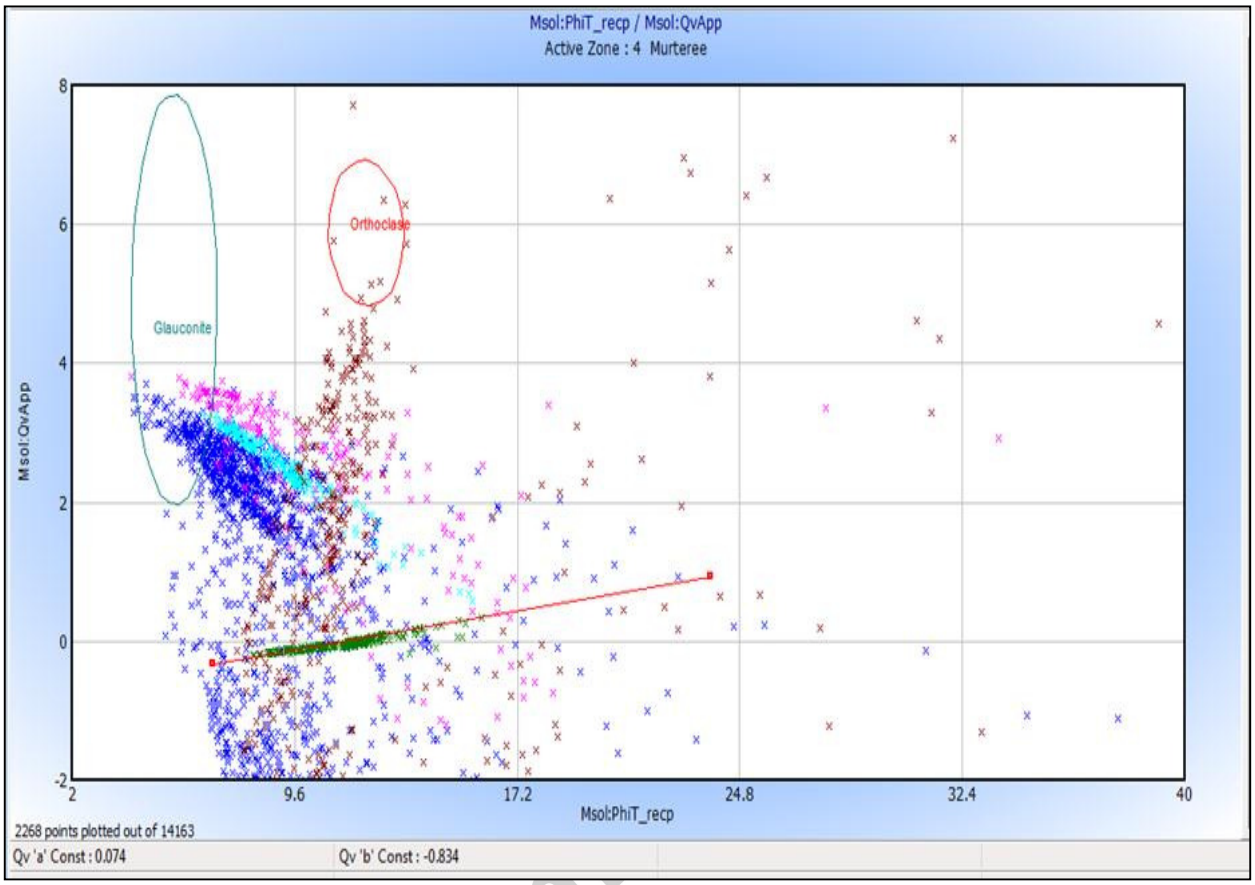

Figure 14: Cross plot between the PHIT and App Qv, a linear relationship can be seen in green water wet interval. Waxman and Smit's 'a' and 'b' are determined by this cross-plot. The blue circle shows area of Glauconite and red circle shows area of Orthoclase. Both the circles are situated at higher Qv value suggesting that both the minerals have Qv higher than other clay minerals. Since the log derived Qv should be correlated to an appropriate porosity measurement in order to define a Qv –ϕT relationship, either in the form of Qv = a ϕT ^-b Or Qv = a/ϕT –b. The obtained relationship is then applied to the hydrocarbon bearing section to calculate Qv.

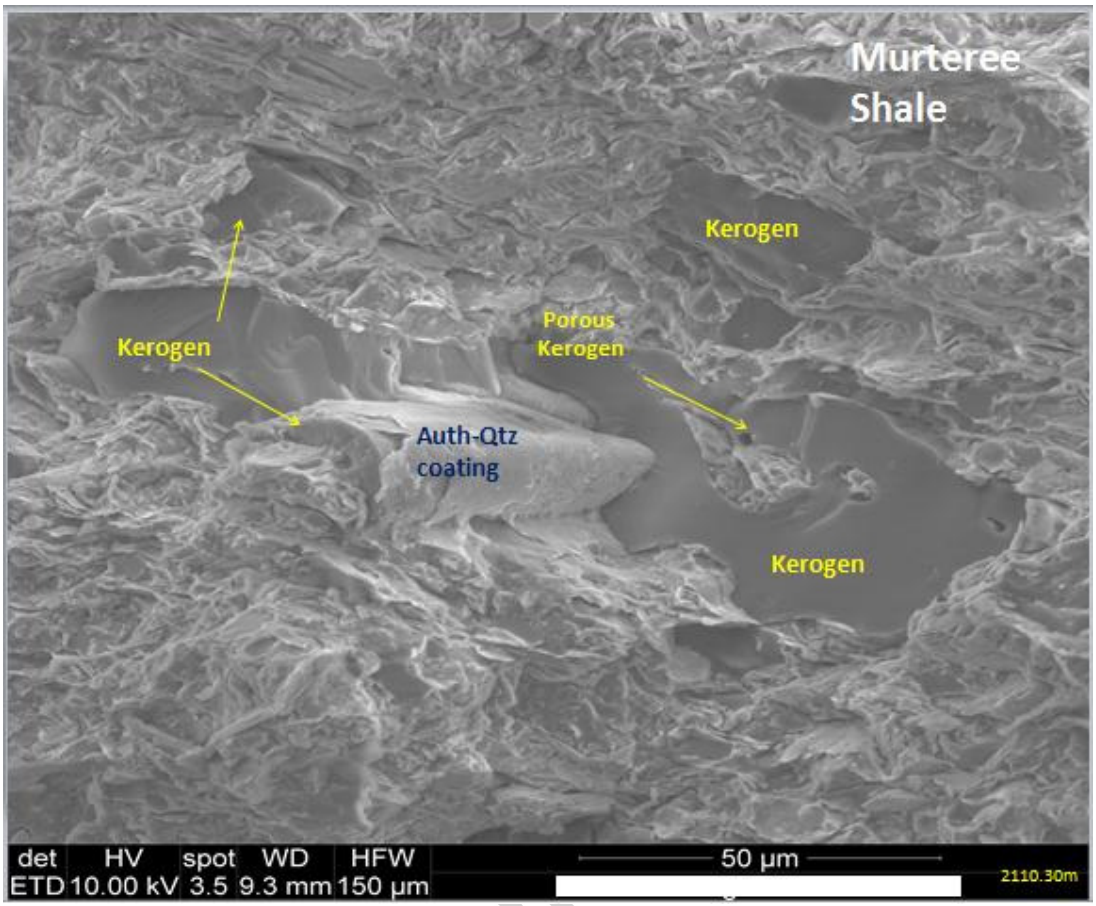

Figure 15: Kerogen embedded in a clay-rich matrix with low porosity in the Murteree Shale in Dirkala-2 well. Open pores measure from 10-50 nm to ~ 2 µm. Some authigenic quartz coatings are observed (Jadoon et al., 2016)

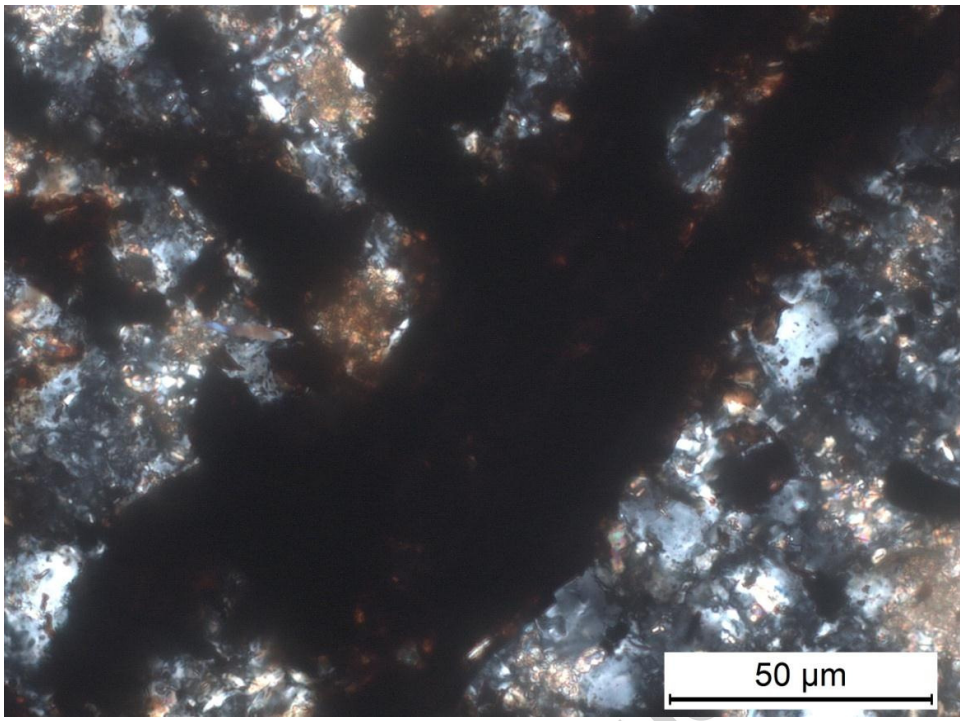

Figure 16: Photomicrograph of an organic rich shale in Murteree Dirkala-2 showing well-opaque organic material nearly 2mm wide. Cross Polarized light (60X).

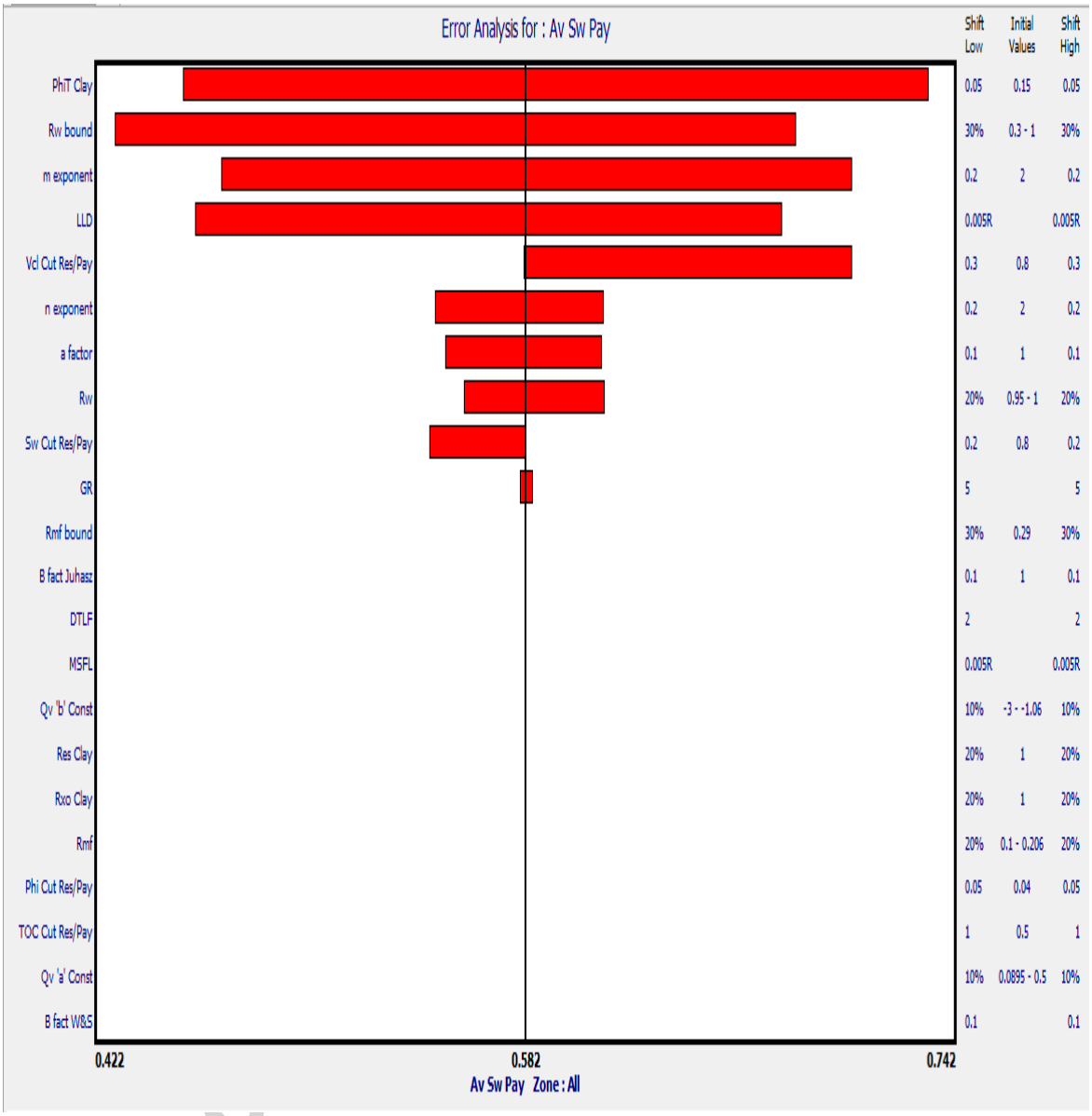

Figure 17: shows the impact of the uncertainty of each variable used in the uncertainty analysis. The Tornado chart show that that the largest impact on the water saturation (Sw) calculation is of Porosity of shale and bound water resistivity, followed by m exponent and resistivity respectively. This further supports the idea of getting special core analysis (SCAL) to determine core derived CEC, electrical properties (a,m & n) to calculate Sw with better accuracy.

.